The expression of Neuroserpin and its role in neonatal hypoxic-ischaemic encephalopathy

Jan Fischer

Student Number: 1033937
University of Oxford
Department of Physiology, Anatomy and Genetics
Supervisors: Prof. Zoltán Molnár and Dr. Anna Hoerder-Suabedissen

Abstract

Background: Perinatal hypoxic ischaemia is one of the most prevalent causes of neonatal morbidity and mortality worldwide. Hypothermia is currently the only available treatment option. Neuroserpin, an inhibitor of tissue plasminogen activator and an endogenously secreted protein, has been shown to result in a reduction in brain damage and overall functional improvements in models of adult cerebral infarction (Millar et al., 2017). It has therefore been hypothesised that it may also reduce damage caused by perinatal hypoxic ischaemia.

Methods: We studied a Neuroserpin knock-out mouse (Madani et al., 2003) to shed light on potential neuroprotective properties that this protein may possess. A modified Rice-Vannucci model was employed (Rice et al., 1981) which involves unilateral carotid artery ligation with subsequent 40 minutes of hypoxia to induce hypoxic ischaemic encephalopathy in one brain hemisphere of P8 mice. Mice were sacrificed at P10 and brain sections were stained with Triphenyltetrazolium chloride (TTC) to determine the area of ischaemic damage. Sections of wild-type mice were further used to carry out immunohistochemistry to determine Neuroserpin expression between P4-P14 as well as subsequent to exposure to hypoxic insults. Finally, expression was also explored in a human brain of 38 post-conception weeks (pcw).

Results: Our experiments in the Neuroserpin KO mouse show that Neuroserpin has no statistically significant effect on ischaemic damage following hypoxic-ischaemic injury in the knockout versus the wild-type. When comparing brains exhibiting ischaemic damage as shown by TTC staining, the mean ischaemic volume in the knock-out and wild-type mice were 7.78 mm^3 and 6.71 mm^3 respectively ($p=0.69$, SEM=1.9, $n=25$). The region most vulnerable to damage was the hippocampus followed by the striatum. The thalamus and the cortex showed significantly reduced vulnerability in comparison. In wild-type mice, Neuroserpin shows strong expression in layers 5 and 6 of the cortex and peaks at P8 in layer 6B. There are fewer Neuroserpin positive cells in the subplate of the ligated side in

comparison to the non-ischaemic control side in mice with exposure to hypoxia. Human Neuroserpin expression at 38 pcw most closely resembles that of P10 mice.

Conclusions: Neuroserpin was not shown to possess neuroprotective properties in the mouse model for neonatal hypoxic-ischaemic encephalopathy. The reduction in Neuroserpin expression in hypoxic-ischaemic encephalopathy may be attributed to vulnerability of Neuroserpin secreting cortical layers (McQuillen et al., 2003) as well as tight regulation of expression during neurodevelopment.

Acknowledgements

I would like to express my sincere gratitude to Prof. Zoltán Molnár for always being available for guidance as well as for truly enabling his students to develop personally and professionally thereby promoting the growth of future neuroscientists.

I am very thankful to Dr. Anna Hoerder-Suabedissen who has had a hand in teaching me virtually everything I know about experimental work in rodents and whose patience and continuous support has allowed this project to progress.

It was a delight working with Dr. Kristina Parley who was a constant source of advice and a vital help in trouble-shooting many of the problems encountered. I am also very thankful for the work of Lancelot Millar who provided much of the preliminary results that this project is based on.

I owe much gratitude to my fellow students Jolande Disser and Chrysoula Giasafaki as well as post-doc Dr. Shuichi Hayashi for their professional help and personal support whenever things got difficult.

Further thanks goes to the London, Newcastle and Oxford brain banks for providing human tissue sections. Carolyn Sloan, Hannah Brooks and Prof. Olaf Ansorge at the Oxford Brain Bank have further enabled me to process human tissue sections. Dr. István Adorján has, moreover, provided images of stained human brain sections for which I am very grateful.

Much support was also provided by Angela Curran, Richard Maxwell and Dr. Caroline Bergmann at the Biomedical Sciences Building. Sarah Noujaim has further helped me navigate many of the administrative hurdles.

Finally, I would like to thank my parents, Kerstin Fischer and Dr. Tom Fischer, as well as Ingrid Contreras for their continuous support throughout my endeavours.

Contents

Abstract 1

Background: 1

Methods: 1

Results: 1

Conclusions: 2

Acknowledgements 3

1. Introduction 7

1.1 Neonatal hypoxic-ischaemic encephalopathy 7

1.2 Neuroserpin 9

1.2.1 Structure, function and expression pattern 9

1.2.2 Neuroserpin secretion from the subplate 9

1.2.3 Neuroserpin expression following brain insults 10

1.2.4 Neuroprotective properties of Neuroserpin 10

1.2.5 Mechanisms of neuroprotection 11

2. Materials and Methods 13

2.1 Experimental animals 13

2.2 Modified Rice-Vannucci model 13

2.2.1 Preparation of surgical area 13

2.2.2 Anaesthesia and preparation of mouse pups 13

2.2.3 Surgical common carotid artery ligation 14

2.2.4 Hypoxic chamber 15

2.3 Perfusion 16

2.4 Tissue preparation, staining and immunohistochemistry 17
2.4.1 Triphenyltetrazolium chloride staining 17
2.4.2 Immunohistochemistry 17
2.5 Imaging and image analysis 19
2.5.1 Microscopy images 19
2.5.2 Quantification of Neuroserpin fluorescent immunohistochemistry 19
2.5.3 Neuroserpin immunoreactivity heatmaps 20
2.5.4 Quantification of ischaemic damage 20
2.6 Statistical analysis 21
2.7 Analysis of rat tissue 22
2.8 Analysis of human tissue 22
3. Results 23
3.1 Neuroserpin expression in wild-type mice 23
3.2 Neonatal hypoxic-ischaemia in wild-type and Neuroserpin knock-out mice 27
3.3 Effects of hypoxic-ischaemic encephalopathy on Neuroserpin expression 30
3.4 Potential mechanisms taking over the functions of Neuroserpin in the KO 34
3.5 Comparing neonatal human and mouse Neuroserpin expression 35
4. Discussion 38
4.1 Investigating neuroprotective properties of neuroserpin in neonatal models 38
4.2 Comparison to Neuroserpin's properties in adult stroke models 38
4.3 Region and layer specific susceptibility to damage 40
4.4 Variability of subplate size and neuroserpin expression during development 41
4.5 Comparison to clinically approved treatments for HIE 42
5. Limitations of Methods 44

5.1 Neuroserpin quantification 44

5.2 Rice-Vannucci model and the quantification of ischaemic damage..... 45

5.3 Human tissue stainings 46

6. Bibliography 47

1. Introduction

Neonatal hypoxic ischaemic encephalopathy (HIE) is a neurological condition characterised by abnormal cortical function due to cellular and structural damage of the neonatal brain (Volpe, 2001). This damage is brought about by a lack of oxygen delivery to the brain leading to focal or global hypoxia and ischaemia. Oxygen delivery is most commonly impaired during the perinatal or the immediate neonatal period (Millar et al., 2017). This can be a result of placental dysfunction and insufficiency, inadequate blood flow to the brain or poor oxygen absorption in the neonatal lungs (Bano et al., 2017). Mortality and life-long morbidity, such as movement disorders, learning disabilities and seizures, are frequently the outcomes (de Vries and Jongmans, 2010). Due to the central nervous system's limited ability to regenerate, current therapies focus on reducing the extent of damage caused by the initial insult and the resulting sequalae. The small number of clinically available therapeutic options makes the development of further treatments essential (Davidson et al., 2015). A promising candidate is the endogenously found protein Neuroserpin as it has been shown to have expression in the neonatal brain as well as poses neuroprotective properties. To understand Neuroserpin's potential actions with regards to neonatal hypoxic ischaemic encephalopathy, I will first elaborate on the disease itself and will then present and overview of the existing evidence surrounding the properties and functions of neuroserpin.

1.1 Neonatal hypoxic-ischaemic encephalopathy

Encephalopathy is a general term that denotes a dysfunction of the brain and as such encompasses a wide array of signs and symptoms. The reported incidence of NHIE varies widely because of differing diagnostic criteria between studies and between geographical locations. When comparing multiple population-wide studies the median incidence of NHIE lies at approximately 4 cases per 1,000 live births (Alake et al., 2018). It is however of note that most of these studies report data from more economically developed countries and may thus underestimate the global incidence. It has therefore been suggested that over 1 million infants have been affected worldwide (Lee et al., 2013).

Numerous mechanisms of brain damage have been reported following peri- or neonatal oxygen-glucose deprivation. These revolve around cortical cell death as well as the disruption of cerebral vasculature and the blood brain barrier (Millar et al., 2017). Neuronal cell death is one of the most critical forms of damage due to the limited capacity of postnatal neurogenesis in the human brain (Sorrells et al., 2018). The death of neurons can be the result of programmed and unprogrammed cellular mechanisms which show some correlation with the severity of the injury (Thornton et al., 2017a). Unprogrammed, necrotic cell death increases in prevalence as the severity of the insult increases whereas programmed apoptosis and necroptosis is more prevalent in mild injuries. It has been hypothesized that cell death as a result of hypoxia is brought about by inflammation, excitotoxicity, mitochondrial dysfunction, oxidative stress and endoplasmatic reticulum stress (Millar et al., 2017; Thornton et al., 2017a, 2017b). These can reduce ATP production meaning that energy requirements exceed energy supply (Nair and Kumar, 2018). Treatment approaches have therefore been devised to mitigate these factors.

There is currently only one clinically approved treatment for neonatal hypoxic ischaemia that is therapeutic hypothermia. This involves the cooling of either the entire body or head only to a temperature of 33-34 °C for 72 hours (Azzopardi et al., 2009, Azzopardi et al., 2014, Davidson et al., 2015) to slow the metabolic rate and reduce cellular energy requirements whilst oxygen and glucose delivery to the cells is compromised (Boutilier, 2001). This has resulted in a significant improvement in clinical outcomes yet morbidity and mortality still remain high. Various adjunct therapies have been proposed and clinical studies having been conducted using Erythropoietin and Xenon (Nair and Kumar, 2018). Nonetheless, preliminary results have been variable suggesting that a significant need for further potential treatment options remains. Neuroserpin has been suggested to be such a novel treatment approach and is thus the focus of this project.

1.2 Neuroserpin

1.2.1 Structure, function and expression pattern

Neuroserpin is a member of the serpin (**SER**ine **P**rotease **IN**hibitor) protein family and is highly conserved across species (Kumar and Ragg, 2008; Osterwalder et al., 1996). Its gene, located on human chromosome 3 (3q26), transcribes into a 55 kDa protein consisting of 410 amino acids (Schrimpf et al., 1997). It has been shown to efficiently inhibit tissue plasminogen activator (tPA) which constitutes the main mechanisms through which Neuroserpin regulates cellular processes (Hastings et al., 1997). Although it does not form stable complexes with other plasminogen activators such as urokinase plasminogen activator it can still affect their expression through interactions in the inflammatory cascade (Cinelli et al., 2001). It shows low levels of expression in the adult heart and testes as well as in the foetal liver and kidney yet is primarily expressed in the vertebrate brain and is particularly found in neurons (Hastings et al., 1997; Osterwalder et al., 1996; Ruegg et al., 1989).

1.2.2 Neuroserpin secretion from the subplate

Neuroserpin, initially named axonin-2, was first discovered as a secreted protein from the dorsal root ganglia of chicken embryos (Osterwalder et al., 1996; Ruegg et al., 1989; Stoeckli et al., 1989). Particularly notable was that it showed expression in neurons but not in glial cells in culture (Ruegg et al., 1989). Significant neuronal expression was also confirmed using single cell RNA sequencing (Adorján et al., 2019). Neuroserpin's profile as a secretory protein was further strengthened by the observation that it is found in large dense core vesicles (Ishigami et al., 2007). Particularly, Neuroserpin secretion from the subplate would be a focus. The subplate is a transient layer of the developing cerebral cortex of mammals (Hoerder-Suabedissen and Molnár, 2015). It houses some of the most mature cells and plays an important role in corticothalamic connectivity. Neurons in the P8 mouse subplate layer were shown to poses functions seen in secretory cells such as well-developed rough endoplasmic reticula (ER) and evidence of ER stress (Kondo et al., 2015). In conjunction with a notable elevation of Neuroserpin levels in the subplate in comparison to other cortical layers it was

determined that Neuroserpin was one of the many factors secreted by the subplate. The subplate's secretory properties have, however, been reported to cease during adult life (Kondo et al., 2015).

1.2.3 Neuroserpin expression following brain insults

In adult rats, Neuroserpin protein levels were shown to be upregulated in the cortical zone surrounding ischaemic lesions as well as in the hippocampus of the lesion side (Yepes et al., 2000). Protein expression peaks at 48 hours following the insult and remains detectably elevated for seven days. mRNA levels of Neuroserpin measured during the first day following middle cerebral artery occlusion (MCAO) were also shown to be elevated (Liang et al., 2004). However, interestingly diabetic rats that show worse ischaemic outcomes following MCAO displayed a less sustained increase with mRNA values returning to baseline after 11 hours. Despite this tPA mRNA levels were unaffected by this variation in Neuroserpin mRNA and remained equally elevated in both the wild-type and diabetic group. Yet, a downregulation of Neuroserpin one and four days after traumatic brain injury in an adult rat model has also been reported (von Gertten et al., 2005).

1.2.4 Neuroprotective properties of Neuroserpin

Potential neuroprotective effects of Neuroserpin have been test in *in vitro* and *in vivo* model systems. *In vitro*, neurons harvested from E15/16 rat embryos undergoing oxygen-glucose deprivation showed greater viability when being exposed to Neuroserpin (Ma et al., 2012). These findings were also replicated in neonatal rat neuron cultures showing reduced apoptosis (Yang et al., 2016). Neuroserpin does not only have protective effects on neurons but also on neonatal rat astrocytes in culture following oxygen-glucose deprivation (Wang et al., 2015).

In vivo, increases of Neuroserpin levels in the brain either through intra-cerebral injections of exogenous protein or through transgenic modifications were shown to significantly reduce ischaemic volume following middle cerebral artery occlusion (MCAO) in adult male rats and mice by 64% and 73% respectively (Cinelli et al., 2001; Yepes et al., 2000). A reduction in apoptotic cells surrounding the ischaemic core of the hypoxic lesion was also reported in vivo (Yepes et al., 2000) although this

anti-apoptotic affect was not consistently found in vitro (Lebeurrier et al., 2005). Finally, population-wide analysis, initially suggested that intronic mutations of the SERPINI1 gene were associated with a higher risk of ischaemic stroke in certain population subgroups, however, these were later called in question (Cole et al., 2007; Tjärnlund-Wolf et al., 2011).

1.2.5 Mechanisms of neuroprotection

Neuroserpin is believed to convey neuroprotective effects through a variety of ways. These have usually been suggested to be tissue plasminogen activator (tPA) dependent. Nonetheless, it is important to not that some evidence has been generated highlighting that Neuroserpin may also have protective properties independent of tPA (Cheng et al., 2017) as a Neuroserpin induced reduction in apoptosis was observed in tPA knock-out mice (Gu et al., 2015). tPA is an endogenously found factor that plays an important role in thrombolysis and is therefore frequently used as a treatment for ischaemic stroke (Yepes et al., 2009). tPA may, however, also have harmful effects following hypoxic-ischaemic insults by increasing inflammation and excitotoxicity as well as disrupting the blood-brain barrier (Yepes et al., 2009).

Neuroserpin is thought to have a neuroprotective effect due to a reduction of inflammation through its inhibition of tPA (Cinelli et al., 2001; Gelderblom et al., 2013). A reduction in activated tPA results in fewer activated microglia which in turn also leads to decreases of microglial derived tissue and urokinase plasminogen activator (Cinelli et al., 2001). Adult Neuroserpin KO mice show substantially increased TNF-α secreting microglia in the hemisphere affected my MCAO versus the control side (Gelderblom et al., 2013). Neuroserpin does not only affect the inflammatory response by reducing TNF-α expression but also by inhibiting other important pro-inflammatory elements such as nitrous oxide, IL-1β or the NF-κB and MAPK pathway (Wang et al., 2015; Yang et al., 2016).

Secondly, neuroprotective properties may also be conveyed due to amelioration of NMDA induced excitotoxicity that plays an important role in ischaemic injury (Lebeurrier et al., 2005; Ma et al., 2012). Reduction of NMDA neurotoxicity due to Neuroserpin exposure was found both *in vitro* and *in vivo*

(Lebeurrier et al., 2005; Ma et al., 2012). Intracortical co-injection of NMDA and Neuroserpin leads to a 50% reduction in cortical ischaemic lesion sizes in mice in comparison to NMDA injection alone (Lebeurrier et al., 2005). Nonetheless, protective properties could only be elicited for NMDA but not for AMPA excitotoxicity (Lebeurrier et al., 2005).

Thirdly, Neuroserpin may effect oxidative stress by reducing the damage caused by reactive oxygen species following hypoxic-ischaemia (Cheng et al., 2017). Apoptosis in primary rat brain cultures following hydrogen peroxide (H_2O_2) exposure was attenuated by administration of Neuroserpin through enhancement of the AKT pathway shown to be important for cell survival (Cheng et al., 2017).

As Neuroserpin is able to ameliorate important mechanisms leading to neuronal cell death it has been hypothesized that Neuroserpin secretion by subplate neurons has a neuroprotective effect on the surrounding tissue and could therefore reduce damage during in utero, perinatal and early neonatal hypoxic injury. This hypothesis forms the basis of our experimental work and is the focus of this thesis.

2. Materials and Methods

2.1 Experimental animals

The mice used during this project were of two strains, namely C57BL/6 and Neuroserpin knock-out mice Serpini1^{tm1Dpw} (Madani et al., 2003). Serpini1^{tm1Dpw} were created on a mixed background strain of 129/Sv and C57BL/6JBom using a neo cassette insertion in the second exon. Mice were held and bred in accordance with the project licence and UK Home Office protocols.

2.2 Modified Rice-Vannucci model

To induce hypoxic-ischaemic encephalopathy a modified Rice-Vannucci model was employed. It is named after the authors of a paper from 1981 describing the procedure in P7 Sprague-Dawley rats (Rice et al., 1981) but was first devised by Seymour Levine in 1960 (Levine, 1960). It involved unilateral carotid artery ligation followed by exposure to a hypoxic environment. Rice et al. (1981) further improved and formalised this procedure by determining suitable durations and levels of hypoxia. We applied a modified Rice-Vannucci model that was carried out on P8 mice (Sinha et al., 2018).

2.2.1 Preparation of surgical area

The surgical procedure was carried out in a laminar flow hood to minimise exposure to allergens and to ensure sterility. A sterile surgical field was established using autoclaved drapes over a heat pad to prevent hypothermia during surgery. A Zeiss standing microscope was required for this delicate surgery. Prior to the procedure pups were weighed to ensure that they exceed 3.5 g in weight. This ensured comparability and avoided adverse outcomes.

2.2.2 Anaesthesia and preparation of mouse pups

Pups were anaesthetised using vaporised isoflurane. Induction of anaesthesia was carried out by placing the pups in a small induction chamber and exposing them to an isoflurane-oxygen gas mixture. The optimal induction concentration of isoflurane (Zoetis, 42058/4195) was 3.5% (v/v) at a flow rate of 1L/min. Mouse pups remained in the chamber until they showed no evidence of a righting reflex or other somatic nervous system responses. They were then placed in a supine position with the animal's

snout being placed in a custom anaesthetic adaptor constructed from a 1.5 ml Eppendorf tube to ensure a good seal around the animal's nose and mouth. Once a paw and/or tail pinch did not elicit any responses the pup was deemed to be suitably anaesthetised. The forepaws were fixed to the underlying drape using adhesive tape to prevent alterations of position during the procedure. The jaw, neck and superior chest area were then sterilised using 670 µl Chlorhexidine Gluconate/Isopropyl applicators (CareFusion, Cat. 270448). A small round hole sterile drape was placed over the animal to prevent contamination of the surgical site. During the procedure the anaesthesia was progressively reduced to enable a swifter post-operative recovery. Following skin incision isoflurane levels were decreased to 2.5% (v/v) and were further dropped to 1.5% (v/v) following artery ligation.

2.2.3 Surgical common carotid artery ligation

The ligation was always carried out on the animal's left common carotid artery (**Figure 1**). An incision was made using curved-sharp dissecting scissors and blunt-nosed serrated forceps to avoid skin damage. The incision was positioned 1 mm left from the midline just superior to the rib cage and was extended superiorly along the anterior neck for 5 mm. Blunt dissection of the superficial facia, adipose tissue and glandular tissue was carried out using micro-dissecting forceps. Despite the incision site being away from the midline, blunt dissection was undertaken over the midline in order to avoid injuring any vasculature supplying adipose and glandular tissue. Vasculature across the midline was sparser than laterally. The sternocleidomastoid muscle, running inferomedially to superiolaterally was then visualised. It was pushed towards the outer wound edge to expose jugular vein and the common carotid artery posteromedially to the vein. Further delicate dissection was required to fully expose these two vessels. Despite the close vicinity of the vagus nerve to these structures it was rarely observed due to its small comparative size. A blunted needle was used to carefully lift the vessels out from the surrounding tissue. Due to its lower pressure the jugular vein was usually occluded, whereas the carotid artery continued to pulse allowing for identification of the vessels. The carotid artery was ligated using a 6-0 vicryl suture (Ethicon, W9981). The ligated vessel was then reburied in the surrounding adipose tissue and the skin incision was closed with a single 4-0 PROLENE suture (Ethicon,

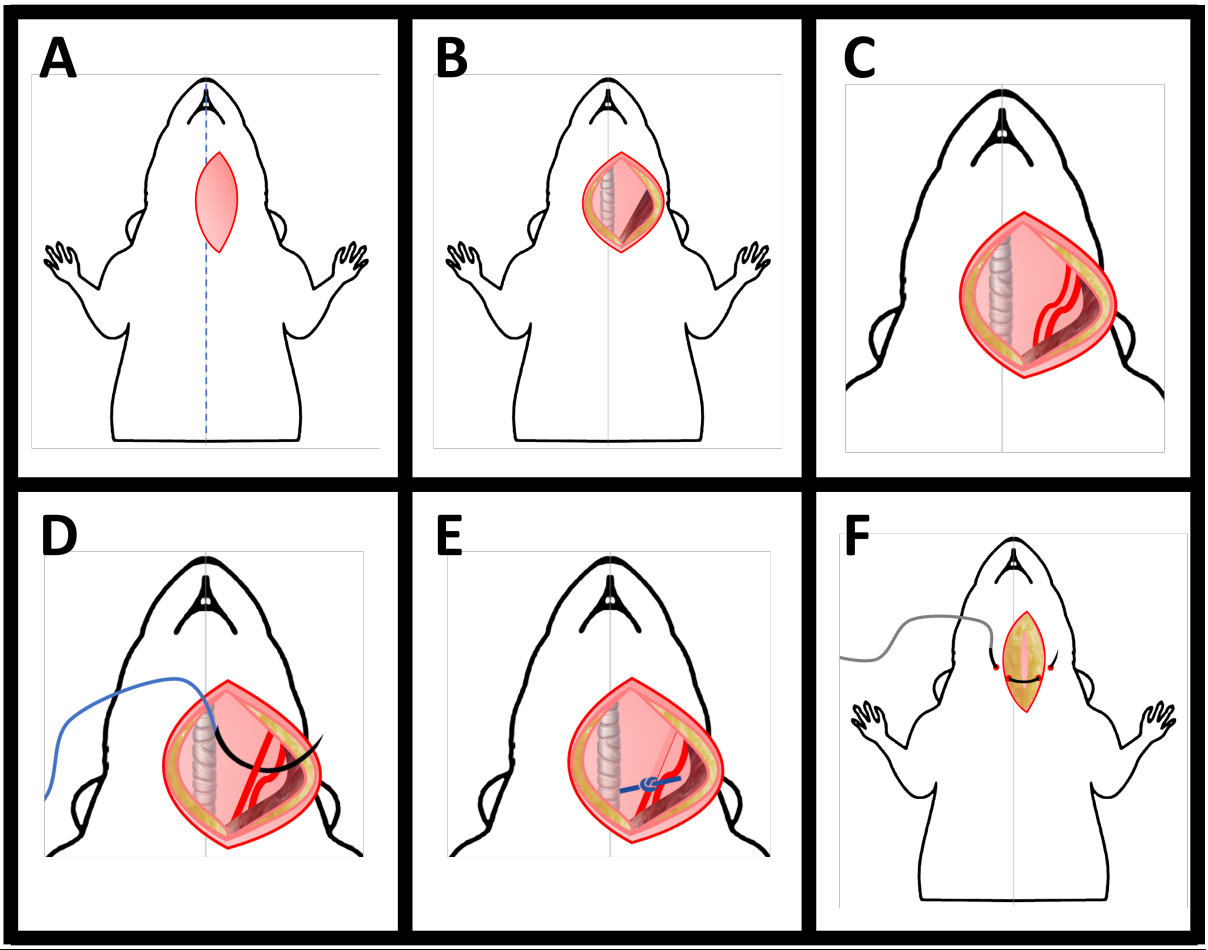

Figure 1. *Diagrammatic representation of carotid ligation as part of the Rice-Vannucci model of neonatal hypoxic ischaemic encephalopathy.* ***A.*** *Skin incision 1 mm lateral of midline.* ***B.*** *Exposing the sternocleidomastoid muscle.* ***C.*** *Exposing left common carotid artery(medially) and jugular vein (laterally).* ***D-E.*** *Ligation of common carotid artery using 6-0 suture with blunted needle.* ***F.*** *Skin closure using single 4-0 PROLENE suture.*

MPP2860). The isoflurane anaesthesia was subsequently stopped and the animal was allowed to recover being given 100% oxygen. Once voluntary motor function was observed the pup was placed in a 37 °C warming chamber in order to further recover. Surgery was usually carried out in batches of three mice where possible. Following this, pups where placed back into the cage with the dam for at least two hours prior to hypoxic chamber exposure.

2.2.4 Hypoxic chamber

Before undergoing exposure to hypoxia, the pups were checked for good movement, wound closure and absence of wound discharge. The hypoxic chamber consisted of an individually-vented mouse cage (IVC) that had been modified to reduce airflow into and out of the cage. A hose was inserted that would allow for the delivery of gas into the chamber. This setup was placed into a water bath heated

to 37 °C to prevent hypothermia during hypoxia. Temperature and humidity could further be monitored from within the chamber using a wireless thermometer. As adverse effects were reported over 35 °C this temperature was never exceeded inside the chamber. The pups were checked every 5 min. for signs of distress which include unprovoked squeaking, significant reduction in respiratory rate and seizure-like activity. Once they displayed any of these signs the procedure would be terminated and the animals would be culled. To maintain good rates of survival the hypoxic time was limited to 40 min. for pups that had previously undergone unilateral carotid artery ligation. A second cohort of mouse pups underwent 90 min. of hypoxia but had no prior carotid ligation.

2.3 Perfusion

Perfusions of mice were usually undertaken at P10, 48 hours following the Rice-Vannucci procedure. A peristaltic pump was used to transcardially perfuse the mice with 6 ml of 0.1M phosphate buffered saline (PBS, pH7.4) and/or 4% (v/v) paraformaldehyde (PFA) (Sigma, F8775). Mouse pups were terminally anaesthetised with an intraperitoneal injection of 0.1 ml Pentobarbitone Sodium 20% (w/v) (Animalcare UK, XVD135). Once no somatic nerve response could be elicited with a paw and tail pinch, the mice were fixed on a Styrofoam block and placed on a perfusion table. A transcutaneous midsternal incision was made to expose the anterior chest wall. This was followed by a transverse subcostal cut being made using dissection scissors through the abdominal skin, fascia and muscles of the animal taking care to avoid injury to the abdominal organs. The cut was then bilaterally extended upwards along the anterior axillary line bisecting the ribs. The first rib was left intact to prevent damage to the subclavian artery and vein that could result in premature exsanguination. The diaphragm was opened from below using blunt dissection thereby allowing the anterior rib cage to be levered upwards exposing the thoracic organs. At this point cardiac systole and diastole could still be observed. A 27-gauge 13 mm needle was inserted into the left ventricle of the heart followed by a cut into the right atrium thereby allowing for a slow perfusion with PBS with the aim of washing out the majority of the blood from the vasculature. Once the discharge from the cut right atrium had cleared, PBS perfusion was ceased. Unless the brain tissue was to be used for Triphenyltetrazolium chloride

(TTC) staining brains were further perfused with 4% (v/v) paraformaldehyde for 90 sec. Surgical decapitation between the spinal cord levels C5-C7 was undertaken. A transcutaneous sagittal midline cut was made across the head to expose the skull. A second cut with the same orientation was then used to open the skull using micro-dissecting scissor commencing at the occiput and continuing towards the nasal bones. The two skull halves were bent outwards to allow for the extraction of the brain using a small surgical spatula.

2.4 Tissue preparation, staining and immunohistochemistry

2.4.1 Triphenyltetrazolium chloride staining

To demarcate areas of ischaemic injury 2,3,5-Triphenyltetrazolium chloride (TTC) (Sigma, T8877) was used. TTC is a mitochondrial marker showing metabolic cellular activity (Mathews et al., 2000). Absence of red TTC staining therefore signifies cell death. Brains designated for TTC staining were cut into four 1.5 mm thick coronal sections using a scalpel and were then immediately place into a bijou tube containing a 2% (w/v) TTC (in 0.1 M PBS, pH 7.4) solution for 25 min. at room temperature. Sections then underwent three 10 min. washes in 0.1 M PBS and were then post-fixed in 4% (v/v) PFA for 48 hours. They were then washed in PBS and imaged following which they were stored in PBS with 0.05% (v/v) sodium azide (PBSA).

2.4.2 Immunohistochemistry

Brains for immunohistochemistry were obtained following perfusions with 4% (v/v) parafolmaldehyde (PFA) as described above. These brains were further fixed for 48 hours in PFA and where subsequently washed in PBS and stored in PBSA. They were cut using a vibrating microtome (Leica VT 1000S) into coronal sections of 80 µm thickness after being embedded in 5% (w/v) agarose (Bioline, BIO-41025). Sections containing anterior S1 sensory cortex were selected and placed in 24-well plates. Three short washes of PBS with a duration of five minutes each followed to remove any azide residues. Sections were put into 2% (v/v) donkey serum (Sigma, D9663) and 0.2% (v/v) triton X-100 (BDH) blocking solution for two hours and then placed in a solution of up to three primary antibodies and block at the

dilutions specified in Table 1. Overnight incubations of 18 hours were carried out. A further three 10-minute PBS washes took place to remove unbound primary antibodies. A two-hour incubation of both secondary antibodies (see Table 2) and DAPI (4', 6-diamidino-2-phenylindole; Sigma, D9542) in blocking solution followed with a final three 10-minute PBS washes to complete the immunohistochemistry protocol. This protocol was adhered to for most primary antibodies with minor alterations when using CTGF (connective tissue growth factor) primaries by increasing the triton X-100 content in the blocking solution to 0.5% (v/v). Where unmatched independent samples were to be compared, control and test sections were processed at the same time in separate wells to reduce process variation. Sections were imaged within 48 hours of protocol completion.

Target	Host	Clonality	Manu-facturer	Product Code	Lot number	Dilution
Connective tissue growth factor (CTGF)	Goat	Poly	Santa Cruz	Sc-14939	C3016	1:1000
Glial fibrillary acidic protein (GFAP)	Rabbit	Poly	DAKO	Z0334	00019620	1:500
Neuroserpin	Rabbit	Poly	Abcam	ab33077	GR32122 85-2	1:1000
Neuroserpin	Goat	Poly	Abcam	ab32901	GR88474-21	1:1000
NeuN	Mouse	Mono	Chemicon	MAB377	2819579	1:1000
Plasminogen activator inhibitor-1 (SERPINE1)	Rabbit	Poly	Proteintech	13801-1-AP	00049446	1:250-1:1000
Protease nexin-1 (SERPINE2)	Rabbit	Poly	Proteintech	11303-1-AP	00014298	1:250-1:1000

Table 1. Description of primary antibodies used during immunohistochemistry experiments

Target	Host	Fluoro-phore	Manu-facturer	Product Code	Lot number	Dilution
Rabbit	Donkey	Alexa488	Life Technologies	A21206	1874771	1:500

Rabbit	Donkey	Alexa568	Life Technologies	A10042	1668655	1:500
Goat	Donkey	Alexa488	Life Technologies	A11055	1627966	1:500
Goat	Donkey	Alexa568	Life Technologies	A11057	1485187	1:500
Mouse	Donkey	Alexa647	Life Technologies	A31571	1757130	1:500

Table 2. Description of secondary antibodies used during immunohistochemistry experiments

2.5 Imaging and image analysis

2.5.1 Microscopy images

TTC stained tissue was imaged using a dissecting microscope (Leica, MZ FLIII) with attached digital colour camera (DFC490, Leica). Of the four sections obtained from each brain only the medial two were imaged. These sections were imaged from both sides. Images of fluorescent immunohistochemistry samples where taken on a laser scanning confocal microscope (Zeiss, LSM 710).

2.5.2 Quantification of Neuroserpin fluorescent immunohistochemistry

Image analysis was undertaken using the open-source software ImageJ (Schindelin et al., 2012). Quantification of Neuroserpin immunoreactivity was conducted blinded and semi-automatically to prevent observer bias and ensure consistency. Due to the strong expression of Neuroserpin throughout the cytoplasm of cells and the distinct nature of fluorescent neurons this approach yielded very accurate results that were verified through manual counts. For counts restricted to the subplate, an area of 75-125 µm (age dependent) on either side of the line of highest subplate fluorescence was selected (**Figure 2**). This ensured that all subplate cells would be taken into account. Some Neuroserpin positive neurons in the overlaying 6a cortical layer fell into this region. Yet, due to the high fluorescent cell numbers in the subplate these had little impact on overall cell numbers. Images were then converted to binary images using a sample specific threshold determined to reduce background noise.

The *analyse particle* plug-in in ImageJ was used to ascertain the number of Neuroserpin positive cells with permissible cell sizes being set at 40-1000 µm² and circularity being undefined.

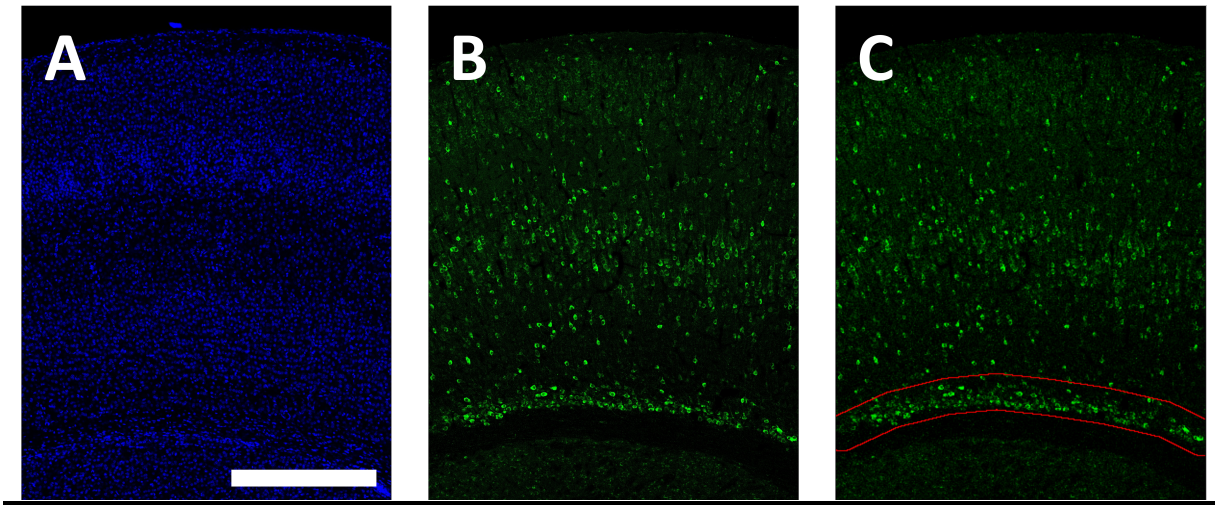

Figure 2. *Subplate neuroserpin quantification.* ***A.*** *DAPI staining (blue) of cross-section of cerebral cortex of P10 mouse. Scale bar equals 500 µm.* ***B.*** *Neuroserpin (green) staining of the same section.* ***C.*** *Neuroserpin (green) staining with subplate selection outlined in red.*

2.5.3 Neuroserpin immunoreactivity heatmaps

Overview images were taken of the entire coronal section of the mouse brain on the confocal microscope. These representative sections showed Neuroserpin immunoreactivity patterns in P4-P14 and adult mice. To obtain an average representation of both halves image registration was employed. Using the ImageJ *bUnwarpJ* registration plugin the relevant sections and their horizontally mirrored duplicates were overlaid using landmarked features to increase accuracy. In order to create a heatmap of Neuroserpin immunoreactivity the two overlaid images were averaged and a subsequent *gaussian blur* (10) was applied.

2.5.4 Quantification of ischaemic damage

The quantification of the ischaemic area (marked by a lack of TTC staining) was again undertaken using ImageJ. For this purpose, the left (ischaemic) and right (control) hemispheres were split and converted to 8-bit grayscale images (**Figure 3**). The external edges of the hemispheres were automatically detected by defining tissue as having a luminance of less than 170 on the 256 level luminance 8-bit scale. The outer tissue edges were removed by moving the borders inwards by a further 100-150

pixels. The overall level of whiteness was then determined in the control hemispheres (right side). Tissue ischaemia was then defined as occurring in those pixels whose luminance (whiteness) was further than three standard deviations from the mean luminance (whiteness) in the control hemisphere. The number of pixels that exceed this luminance level in the ischaemic hemisphere were then quantified to give an area of ischaemia. As all sections had two sides, the ischaemic area on the anterior and posterior side of each section was averaged and then multiplied by the average section thickness of 1.5 mm to determine a volume of ischaemia.

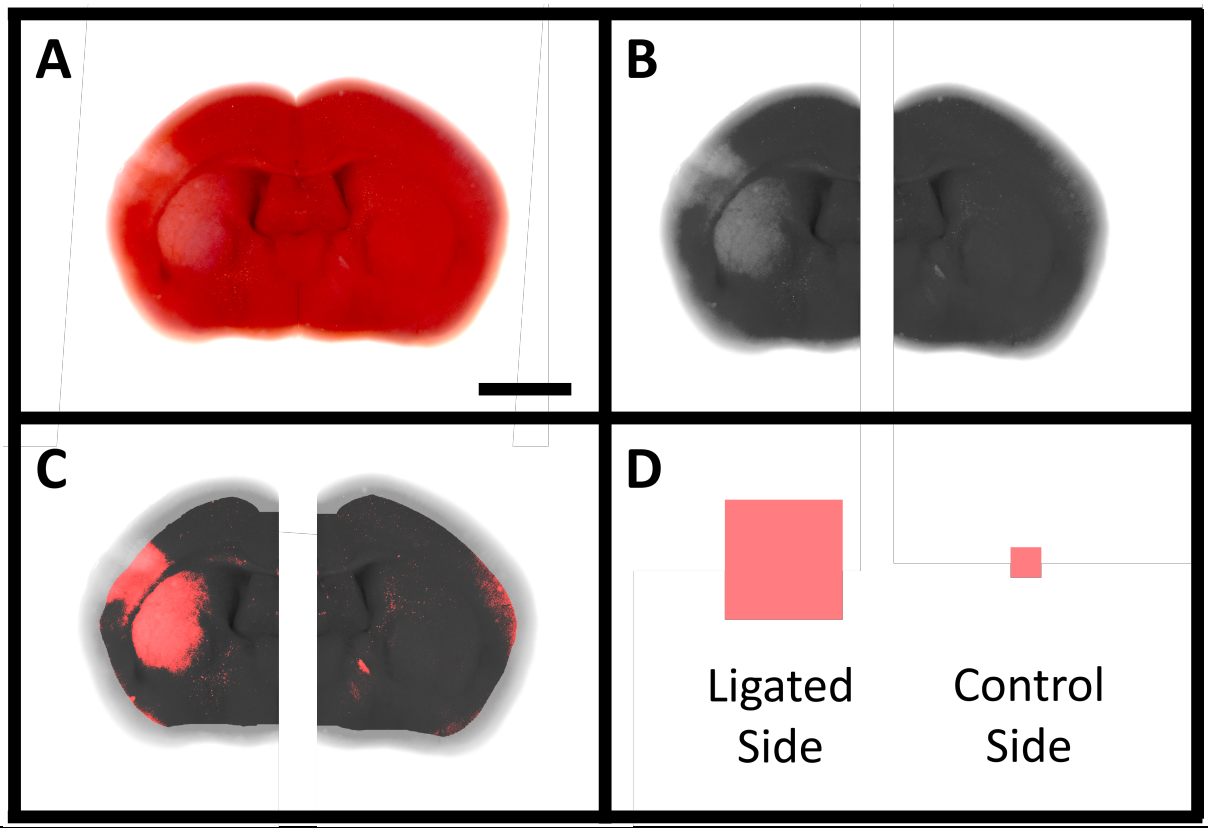

Figure 3. *Quantification of ischaemic damage marked by an absence of TTC.* ***A.*** *Raw image of TTC stained section with mild ischaemia seen in the left hemisphere. Scale bar equals 2 mm.* ***B.*** *Greyscale conversion of section.* ***C.*** *Red area highlights ischaemic area in the ligated hemisphere (left). Ischaemia is defined using non-ligated, control hemisphere and is given as whiteness three standard deviations away from the average pixel intensity of the hemisphere.* ***D.*** *Ischaemic area is calculated by subtracting the area highlighted in the control hemisphere from the one highlighted in the ligated side. Not to scale.*

2.6 Statistical analysis

Data in the experiments conducted was normally distributed allowing for the use of parametric statistical tests. For comparisons of Neuroserpin immunoreactivity in the two hemispheres (ischaemic and control) within single sections a paired-sample two-tailed Student's T-test was used. Where

comparisons were made between expression levels in different animals an independent-sample T-test was employed. Inter-litter variations occurred in experiments comparing hypoxia-only to control animals that were attributed to a new lot of primary Neuroserpin antibody being used. A two-way ANOVA was thus utilised in order to take these variations into account. The level of statistical significance was defined as $p<0.05$ for all tests.

2.7 Analysis of rat tissue

Neuroserpin fluorescent IHC images of brain tissue was obtained from rats that had undergone unilateral hypoxic-ischaemic encephalopathy as per the protocol described by Okusa et al. (2014). Rat tissue was provided by Dr. Truttmann and Dr. Ginet from the University of Lausanne and was stained by Lance Millar (University of Oxford). To summarise, the Rice-Vannucci approach was undertaken two days after birth (P2) with a hypoxic period of 90-120 minutes at 6% oxygen. Brains had been fixed at P8. This tissue was analysed using the same protocols described above.

2.8 Analysis of human tissue

The temporal lobe of an infant at term had been stained for Neuroserpin as well as Alcian-blue and Nissl by Dr. István Adorján (University of Oxford/Semmelweis University). This brain was collected by the London Brain Bank. Alcian-blue, Nissl and Neuroserpin stains were overlaid using the previously mentioned bUnwarpJ ImageJ plugin and the various cortical layers were marked. Neuroserpin positive cells were then quantified in the superior, middle and inferior temporal gyri.

3. Results

3.1 Neuroserpin expression in wild-type mice

To understand the role of Neuroserpin in neonatal hypoxic-ischaemic encephalopathy one needs to first describe its pattern of expression in postnatal mice. The brains of P8 mice are generally accepted to resemble human ones in the late third trimester or neonatal period in terms of developmental stage as the mouse brain continues to develop during the first postnatal weeks (Semple et al., 2013). The expression pattern during the crucial time span of P4-P14 was therefore examined. As the subplate (layer 6b) has been hypothesized to be one of the major sources of secreted Neuroserpin (Kondo et al., 2015), a particular focus was placed on determining Neuroserpin expression in this layer.

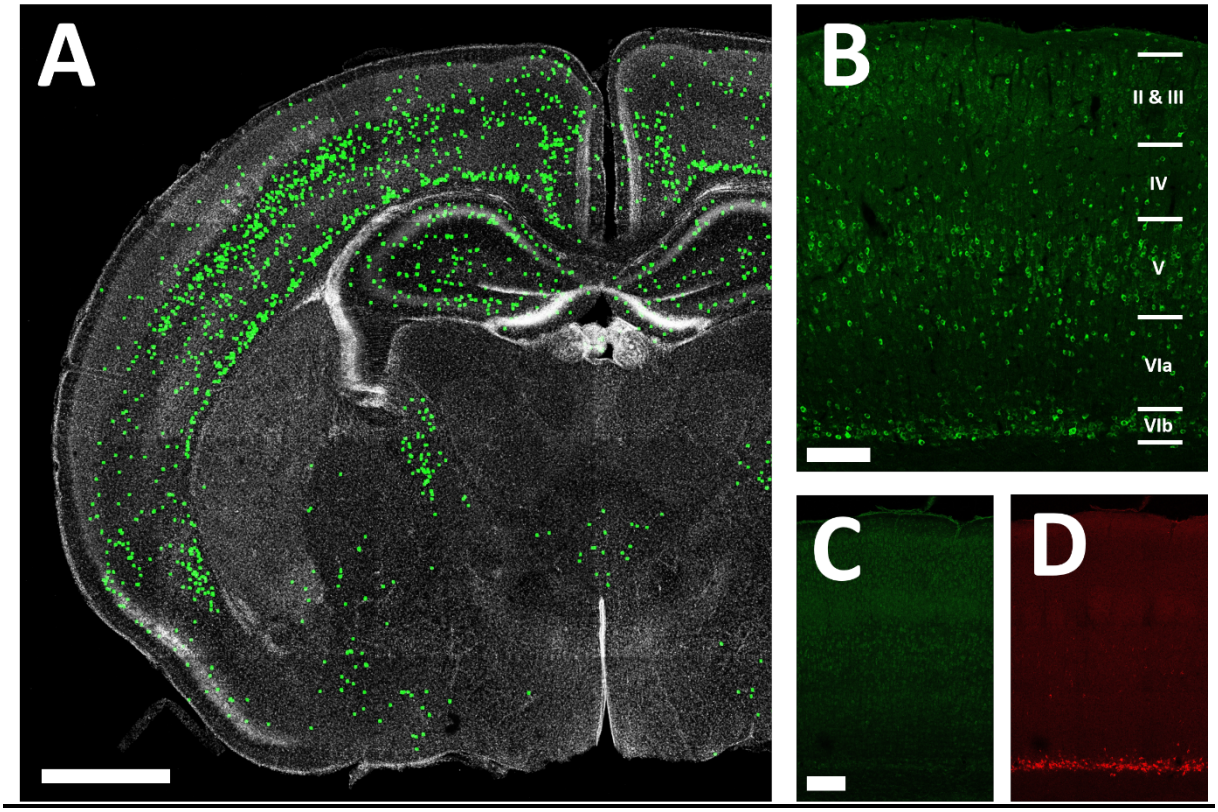

Figure 4. *Fluorescent immunohistochemistry showing Neuroserpin immunoreactivity in a representative P10 mouse brain.* ***A.*** *Neuroserpin positive cells as found in the coronal section of the brain. Markers of individual cells have been enlarged in order to allow for visibility at the given magnification. Neuroserpin immunoreactivity was observed in all cortical layers to varying degrees. Strongest immunoreactivity was observed in layers 5 and 6b. It also shows expression in lateral amygdala and in hippocampal and thalamic cells. Scale bar equals 1 mm.* ***B.*** *Magnified sensory cortex stained for Neuroserpin. Cortical layers marked. Scale bar equals 200 µm.* ***C-D.*** *Neuroserpin KO mouse stained for Neuroserpin (C) and CTGF (D). Only background fluorescence is visible in Neuroserpin stain. CTGF marks subplate (layer 6b) cells. Scale bar equals 200 µm.*

In mice, Neuroserpin is most noticeably expressed in the cerebral cortex but importantly also has further foci of expression in the hippocampus, amygdala and the lateral thalamus (**Figure 4.a**). It can be found in all layers of the mouse cerebral cortex as well as all ages examined in this study ranging from P4-P14 and 6 months old adult mice. Yet, significant differences exist between individual mouse cortical layers. Neuroserpin positive cells are most abundant in layer 6b (L6b) and layer 5 (L5) (**Figure 4.a-b**). Relative scarcity of Neuroserpin immunoreactivity was found in layer 1, 4 and 6a. Aside from

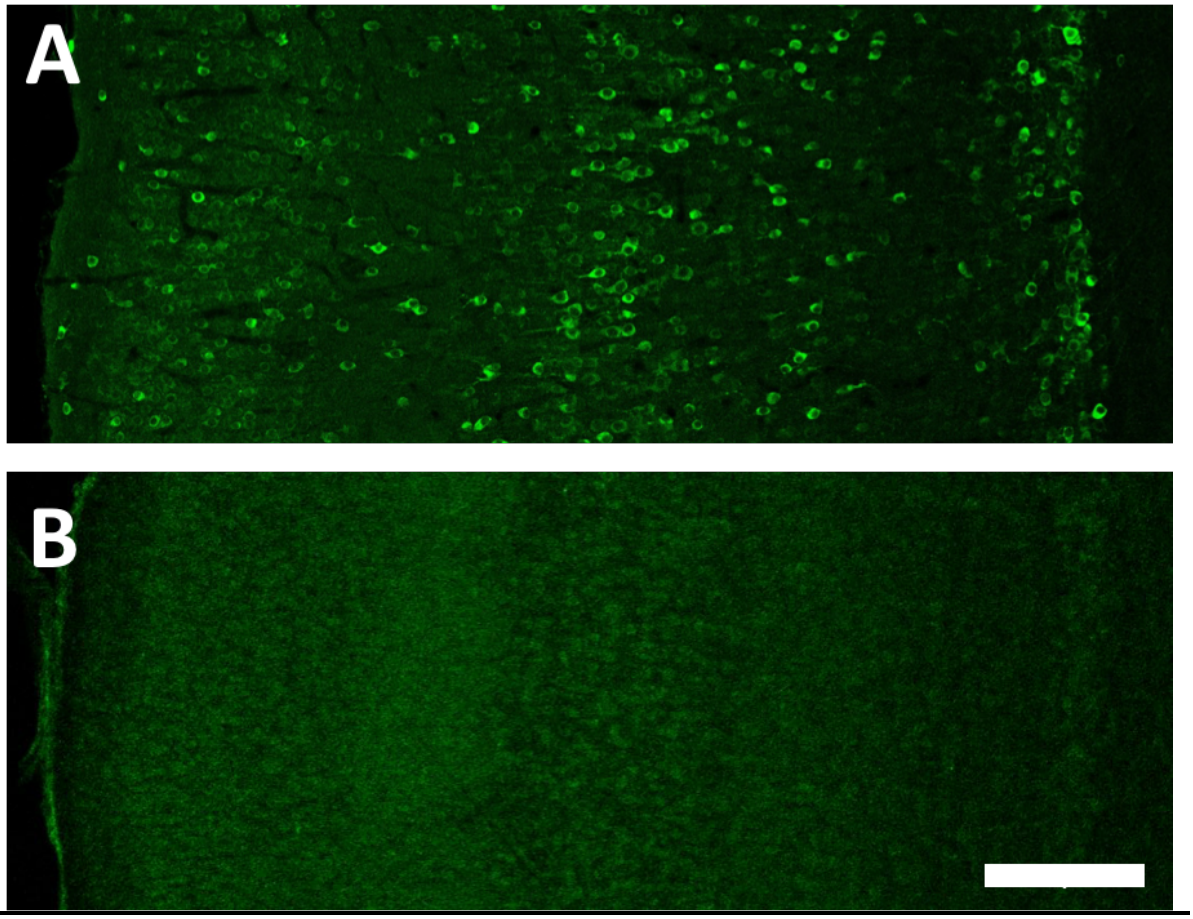

Figure 5. *Neuroserpin KO mouse shows no Neuroserpin protein expression as detected by immunohistochemistry (Antibody used: Abcam, Ab33077).* ***A.*** *Neuroserpin stain (green) WT mouse cortex.* ***B.*** *Neuroserpin stain (green) KO mouse cortex. Only background fluorescence visible. Scale bar equals 200 µm.*

wild-type mice the Serpini1^{tm1Dpw} mice were also examined for Neuroserpin expression (Madani et al., 2003). These Neuroserpin knock-out mice were employed to examine the effects of Neuroserpin in neonatal hypoxic-ischaemic encephalopathy and showed no expression of the Neuroserpin protein in the mouse brain as tested by immunohistochemistry (**Figure 4.c-d & Figure 5**). Furthermore, Western blot previously conducted by others in the lab and employing two different primary antibodies

(Abcam, Ab55587 and Ab32901) detected no Neuroserpin protein in the brain of these knock-out mice (Millar, to be submitted as DPhil Thesis, 2019). No gross anatomical or histological changes were detected in the brains of these mice as previously documented by Madani et al. (2003).

In wild-type mice Neuroserpin expression is not static during the first two postnatal weeks and varies significantly within individual cortical layers. The density of Neuroserpin expressing cells between P4 and P14 is always greatest in L6b (**Figure 6**.**c**). Neuroserpin immunoreactivity peaks at P8 (59.9 cells/0.1 mm², SEM=0.5, n=4) in L6b and decline thereafter. Likewise, cell density in L5 (and L6a) also peak and then decline. This peak in L5 is, however, only reached at a later developmental time point at P10 (55.4 cells/0.1 mm²; SEM=1.8; n=4). Despite the density of Neuroserpin expression being lower in L5 than in L6b, it contains greater numbers of Neuroserpin immunoreactive cells due to its larger size (**Figure 6**.**d**). The total number of Neuroserpin positive cells (NPCs) of L5 is only eclipsed by that of L2/3 at P14 (L5 (at P14): 97.9 cells vs. L2/3 (at P14): 106.4 cells; SEM_{L5}=18.4, $SEM_{L2/3}$=17.6; n=4 brains each). Layers 2/3, unlike 5 and 6b, show a continuous increase in expression from P4-P14. At P4 only 10.2% (SEM=0.9%; n=4) of NPCs in the cortex are found in L2/3, whereas this increases to 29.7% (SEM=2.6%; n=4) at P14 (**Figure 6.e**). The underlying L4 shows the lowest levels of expression of all layers at any time point.

From P4 to P8 the number of NPCs in all of the layers increases proportionally (**Figure 6**.**d**) meaning that the relative ratios of NPCs found in each layer remain similar (**Figure 6**.**e**). At P10 in contrast, the proportion of NPCs in layers 6b and 6a decline whereas they rise in L5 and L2/3. However, by P14 proportions of L5 NPCs also see a fall only leaving L2/3 to have any noteworthy proportional increases.

The peaks in density and proportion of NPCs in layers 6b, 5 and 2/3 are therefore reached at P8, P10 and P14 respectively. Inner layers therefore have earlier maximum densities of Neuroserpin expressing cells than outer layers. This may be evidence of remnant radial migration of Neuroserpin positive cells towards outer cortical layers or an outward wave of sequential activation of Neuroserpin expression in these layers.

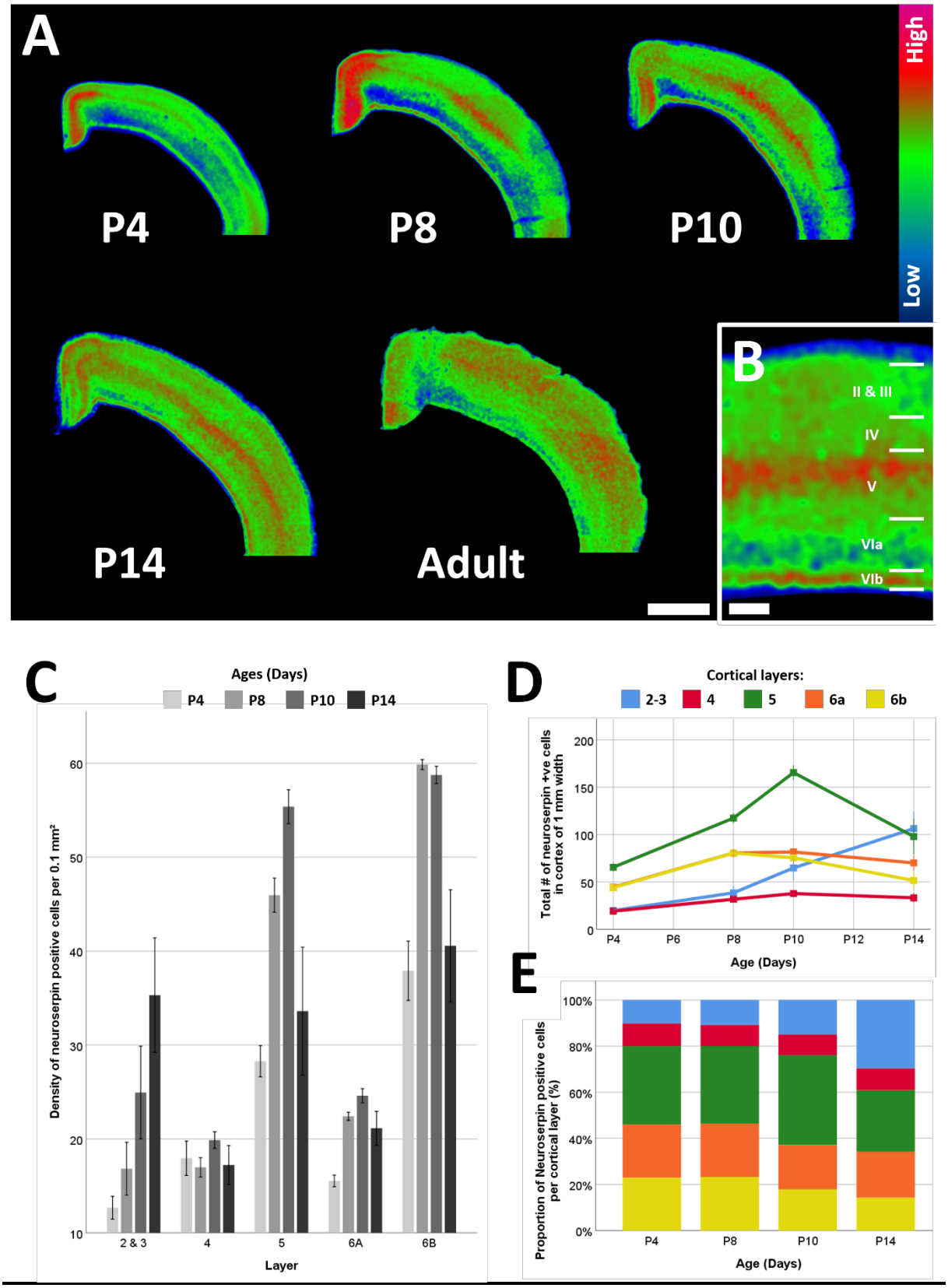

Figure 6. *Cortical Neuroserpin expression changes during postnatal brain maturation.* ***A.*** *Representative heatmaps of Neuroserpin expression of individual animals at the ages specified. Scale bar equals 1 mm.* ***B.*** *Magnified heatmap of sensory cortex Neuroserpin expression in a P10 mouse with cortical layers marked. Scale bar equals 200 µm.* ***C.*** *Density of Neuroserpin positive cells in the various cortical layers of the sensory cortex. Neuroserpin positive cells are most densely located in the subplate (6b) at all the time points examined. Expression peaks in the subplate/L6b at P8 and in L5 at P10. Expression continuously rises in layers 2 & 3. Error bars indicate one standard error from the mean.* ***D.*** *Absolute number of Neuroserpin positive cells per layer in a cortical section of 1 mm in width.* ***E.*** *Relative proportion of the total number of Neuroserpin positive*

cells in each of the layers. Proportions are stable from P4 to P8 but there is a relative reduction in Neuroserpin expressing cells in L6b and a relative increase in 2 & 3 thereafter.

Heatmapping of Neuroserpin levels in individual samples further highlights the changes in overall cortical expression patterns over time (**Figure 6**.**a**). At P4, Neuroserpin shows some enrichment in L6b and L5 and is most markedly elevated in the retrosplenial cortex, the cortical area closest to the midline. At P8 and P10 cortical expression levels increase generally, but a rise in L5 of the barrel cortex is particularly noteworthy. By P14 Neuroserpin becomes more homogenously expressed throughout L5 and relative abundance in layers 2/3 also increases. Finally, in the adult mouse cortex Neuroserpin expression appears more uniformly distributed throughout the upper cortical layers (2-5) and some remnant L6b expression remains.

3.2 Neonatal hypoxic-ischaemia in wild-type and Neuroserpin knock-out mice

To determine whether endogenous Neuroserpin has neuroprotective properties in the modified Rice-Vannucci model of neonatal hypoxic-ischaemic encephalopathy Serpini1 knock-out mice were compared to wild-type mice. Neuroserpin knock-out mice had previously been used and validated by Madani et al. (2003) and were confirmed to show no expression of Neuroserpin in this study using fluorescent immunohistochemistry (**Figure 4**.**d**). Tissue of 29 knock-out and 14 wild-type P10 mice was examined that had successfully undergone the Rice-Vannucci procedure at P8. The degree of ischaemic damage was assessed using 2,3,5-Triphenyltetrazolium chloride (TTC) that marks cells with metabolic activity (**Figure 7.a**). Of the 43 brains, 25 showed evidence of ischaemia (58%) with the incidence varying significantly per surgical litter from 22% to 100% (**Figure 7.b**). Ischaemic damage had a higher relative incidence in the wild-type than the knock-out group (71.4% vs. 51.7% respectively). Chi-square testing determined that this inter-group variation was non-significant ($p=0.22$) and may thus be potentially attributed to the generally high variability observed in ischaemia following the Rice-Vannucci approach.

Ischaemic damage showed a clear pattern of progression, as certain brain regions were significantly more susceptible than others. The first region to be affected was the hippocampus with the first subtle

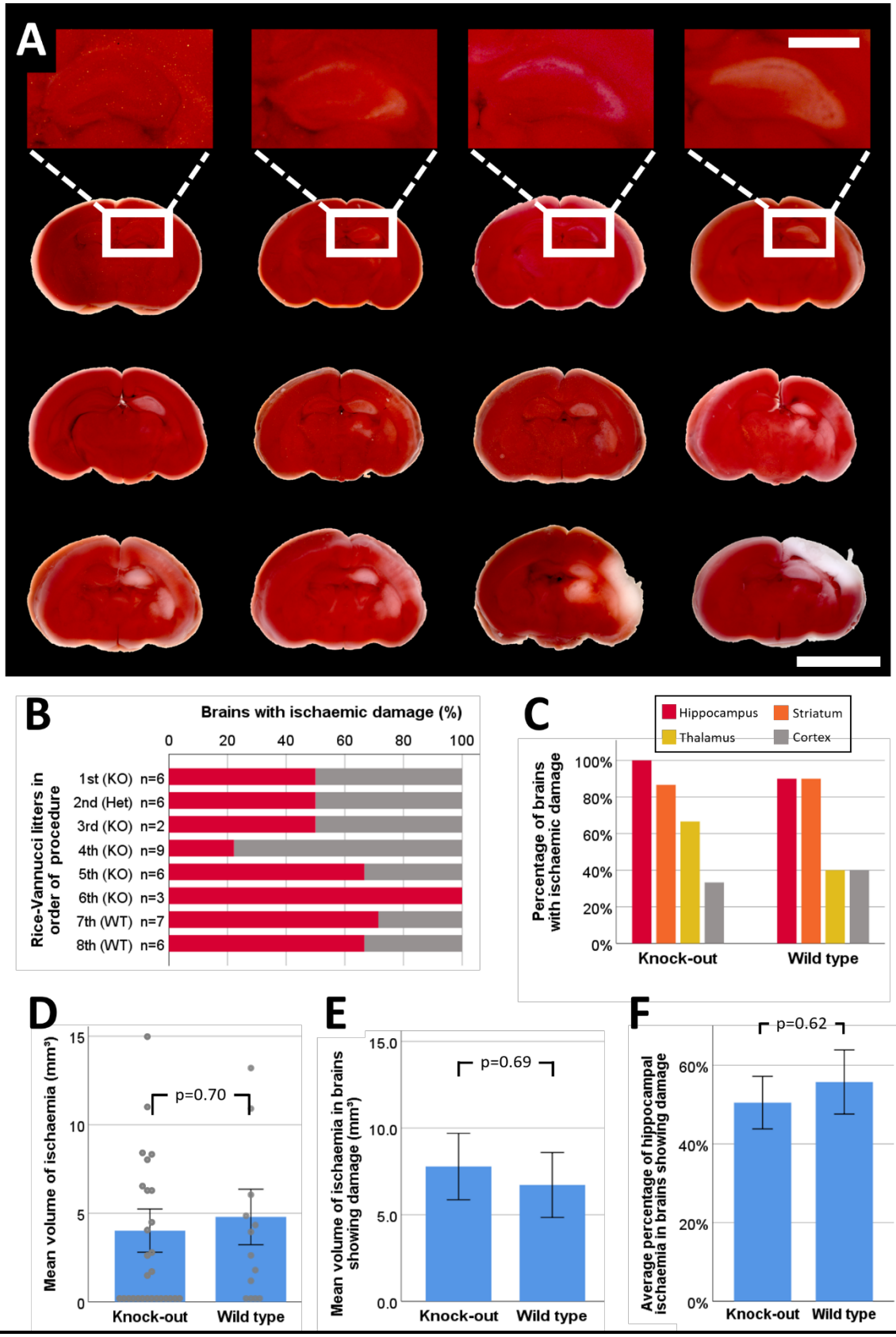

Figure 7. *Ischaemic damage as assessed by TTC staining in P10 mice following Rice-Vannucci procedure at P8 shows no statistically significant difference between KO and WT animals.* ***A.*** *Progression of ischaemic damage. TTC (red) marks viable tissue and its absence signifies ischaemia. The hippocampus is the first region affected followed by the striatum and thalamus. Ischaemia in the cerebral cortex is only seen in severe damage. Scale bar equals 5 mm. Scale bar for magnified hippocampi equals 1 mm.* ***B.*** *Incidence of cerebral ischaemia in each of the litters which underwent the Rice-Vannucci procedure. Litters*

are ranked in order of procedure date. Parental Neuroserpin genotype is stated. The 2nd litter (heterozygous mating) contained 3 KOs, 2 Hets and 1 WT mouse pup. ***C.*** *Likelihood of selected cerebral structures being affected by ischaemia in brains with evidence of damage.* ***D.*** *Mean volume of ischaemia in all brains (n=43) that successfully underwent RV procedure split by Neuroserpin genotype. Error bars indicate one standard error from the mean. Superimposed scatter plot with two points outside of shown range (KO: 31.0, WT: 19.4)* ***E.*** *Mean volume of ischaemia excluding brains without any evidence of damage.* ***F.*** *Mean percentage of hippocampal area affected by ischaemia in brains with damage.*

ischaemic changes occurring in the hippocampal pyramidal cell layer and then spreading to the oriens layer and the CA1-CA3 fields (**Figure 7.a**). 96% of brains exhibiting ischaemic damage showed a degree of ischaemia in the hippocampus (**Figure 7.c**). The striatum had a similar risk with 92% of brains with ischaemia showing damage in this region. The thalamus and the cortex showed substantially reduced vulnerability to ischaemic damage (56% and 36% respectively). The likelihood of damage of the aforementioned areas was largely similar when comparing the knock-out and wild-type groups. Only the thalamus showed a noteworthy increase in the incidence of ischaemia in the knock-out mice (67% KO vs. 40% WT).

The assessment of average ischaemic volumes in the knock-out and wild-type mice yielded no statistically significant differences. Of all mice that successfully underwent the procedure (n=43) the knock-out versus the wild-type group had an average ischaemic volume of 4.02 mm^3 versus 4.79 mm^3 (SEM_{KO}=1.22, SEM_{WT}=1.56; n_{KO}=29, n_{WT}=14; p=0.70) (**Figure 7.d**). Some skew of the data was created by a significant number of brains without ischaemia. When brains with no evidence of ischaemic damage were excluded, to further normalise the data, the order was reversed. The knock-out mice now were trending towards larger volumes of damage than wild-type mice (7.78 mm^3 vs. 6.71 mm^3; SEM_{KO}=1.91, SEM_{WT}=1.87; n_{KO}=15, n_{WT}=10, p=0.69) (**Figure 7.e**). The relative area of hippocampal ischaemia in knock-out and wild-type mouse brains with damage was found to be 50.5% and 55.7% respectively (SEM_{KO}=6.7%, SEM_{WT}=8.2%%; n_{KO}=15, n_{WT}=10, p=0.62) with no statistically significant difference being detected (**Figure 7.f**). Overall, standard deviations in this sample set were particularly high owing to the high variations seen in outcomes of the Rice-Vannucci model.

Post hoc analysis suggests that the standardized effect size of 0.16 standard deviations (SD) requires an extremely large sample size of 619 animals per group in order to reach statistical significance at

80% power using a two-tailed Student's T-test. An effect size of 1.19 SD would be required in order to allow for detection at the given sample sizes (at 80% power). This would require knock-out mice to have had an average ischaemic volume of 14.7 mm^3 whilst wild-type ischaemic damage remained constant. This value has only been exceeded in 2 of the 15 mice in the knock-out cohort showing evidence of ischaemia and is synonymous with sizeable unilateral damage to the cerebral cortex and further forebrain structures as seen in the three most extensively damaged brain sections in **Figure 7.a**. Nonetheless, this also highlights that given a sufficiently large effect size our experimental setup would have been suitable to detect this.

3.3 Effects of hypoxic-ischaemic encephalopathy on Neuroserpin expression

To examine how hypoxic-ischaemic encephalopathy affects Neuroserpin expression in mouse pups, Neuroserpin levels were quantified in L6b of P10 wild-type mouse brains that had undergone the modified Rice-Vannucci procedure at P8 (**Figure 8.a-b**). Different brains where used to the preceding TTC quantifications as the red TTC stain interfered with fluorescent immunohistochemistry. The number of Neuroserpin positive cells was compared between L6b of the ligated and the control side (**Figure 8.d-e**). L6b Neuroserpin expression was lower in the ligated than in the control side (12.8 vs. 17.9 cells/mm of subplate; SEM_L=1.3, SEM_C=1.9; n=10; p=0.048) when comparing all animals used for this experimental approach narrowly reaching statistical significance (**Figure 8.c**). However, when only comparing the hemispheres of animals displaying evidence of ischaemic damage the difference between the ligated and control side was far more pronounced and distinctly more significant (11.7 vs. 20.2 cells/mm of subplate; SEM_L=2.1, SEM_C=1.9; n=6; p=0.005) (**Figure 8.f**). Importantly, the six brains showed no signs of cortical ischaemia, with ischaemic damage being limited to hippocampal and striatal areas. Due to the close proximity of L6b to the hippocampus low levels of ischaemic damage to this layer could not be excluded.

To further explore these results, a small number of images of Neuroserpin-stained rat brains that had also previously undergone the Rice-Vannucci procedure were obtained and stained by Lancelot Millar

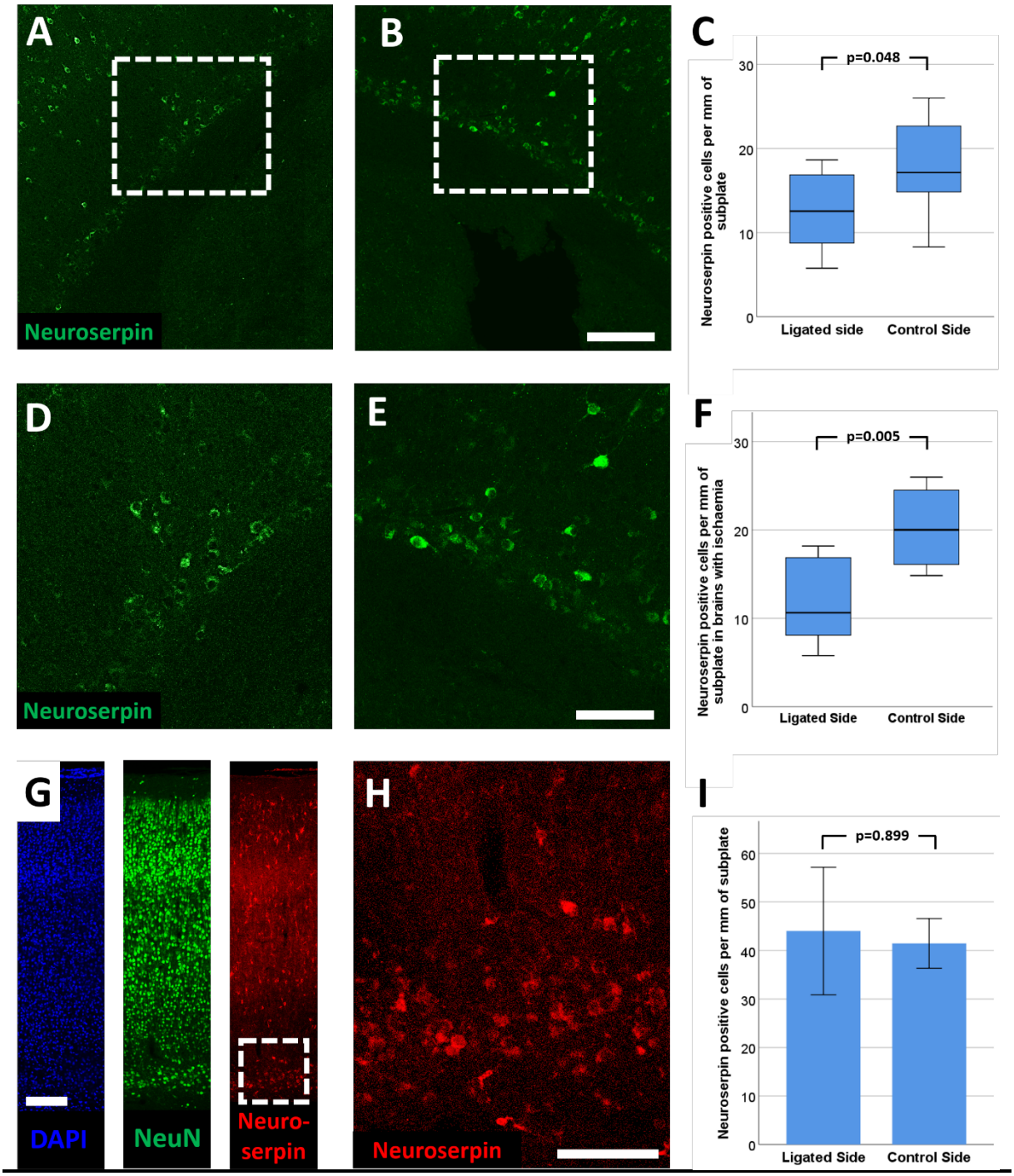

Figure 8. *Neuroserpin immunoreactivity following the Rice-Vannucci procedure is reduced on the cortical side of carotid ligation.* ***A-B.*** *Neuroserpin expression as seen in a representative cross section of the ligated side (A) and unligated side control hemisphere (B). Scale bar equals 200 µm.* ***C.*** *Boxplot of mean number of Neuroserpin immunoreactive cells in L6b of ligated and control hemispheres.* ***D-E.*** *Magnified view of highlighted areas of A and B showing L6b Neuroserpin immunopositive cells in the ligated (D) and the control hemisphere (E). Scale bar equals 100 µm* ***F.*** *Boxplot of mean number of L6b Neuroserpin positive cells in ligated and control hemisphere of brains exhibiting evidence of ischaemic damage.* ***G.*** *Representative images of cross sections of rat cerebral cortex previously having undergone the Rice-Vannucci procedure (at P2, 6% O_2 for 90-120 min., fixed at P8). Scale bar equals 200 µm* ***H.*** *Magnified view of highlighted area of rat Neuroserpin staining in L6b (and lower L6a). Scale bar equals 100 µm.* ***I.*** *Mean number of L6b Neuroserpin positive cells in the ligated and control hemisphere of rat brain tissue.*

(**Figure 8.g-h**). Analysis was conducted in the same manner as that for the mouse tissue. The rat L6b showed no statistically significant difference in Neuroserpin expression when comparing the ligated and the control side (44.0 vs. 41.5 cells/mm of subplate; SEM_L=13.1, SEM_C=5.1; n=3; p=0.899) (**Figure 8.i**). Notably, none of this tissue had been reported to show any gross ischaemic damage in the ligated hemisphere.

The differences in Neuroserpin expression between the ligated and the control hemisphere in the Rice-Vannucci mouse tissue suggested that hypoxia and/or ischaemia might have affected Neuroserpin levels. As numbers of Neuroserpin immunoreactive cells in L6b were particularly decreased in those brains with ischaemic damage, it was hypothesized that severe local hypoxia was responsible for reduced expression. There was, however, uncertainty as to whether tissue necrosis and ischaemia were required for this decrease or whether a hypoxic insult alone was sufficient to reduce L6b Neuroserpin expression. P8 mice were therefore exposed to a hypoxic environment (10% oxygen) for 90 minutes with brains then being collected at P10 as previously in the Rice-Vannucci approach. This was performed on two litters, with littermates acting as non-hypoxic controls. In both litters there was greater L6b Neuroserpin expression in the control group versus the hypoxic group (**Figure 9**.**a**). As two different lots of primary antibody were used, a two-way ANOVA had to be used to compare the hypoxic and control group whilst controlling for litter. The overall Neuroserpin positive cell counts per mm of subplate in the hypoxic and the control group amounted to 49.3 and 57.4 cells respectively (n=9 each, p=0.028). This difference was statistically significant.

Although none of the hypoxia-only brains showed any evidence of ischaemia, more subtle damage to tissue architecture and cellular structure may have caused these changes in expression. In order to show that such subtle changes can be detected in samples with differing Neuroserpin expressions, two of the brains exposed to 90 minutes of hypoxia were selected. The first one was the brain within the hypoxia-only cohort that exhibited the lowest level of Neuroserpin expression whereas the second brain was the one with the highest levels of expression. Sections from these brains were then stained

for glial fibrillary acidic protein (GFAP). This is a marker of astrogliosis, that is frequently seen as a response to central nervous system injury (Sofroniew, 2009). The areas that were co-labelled with GFAP and CTGF (connective tissue growth factor), a marker of L6b, were then quantified to give a

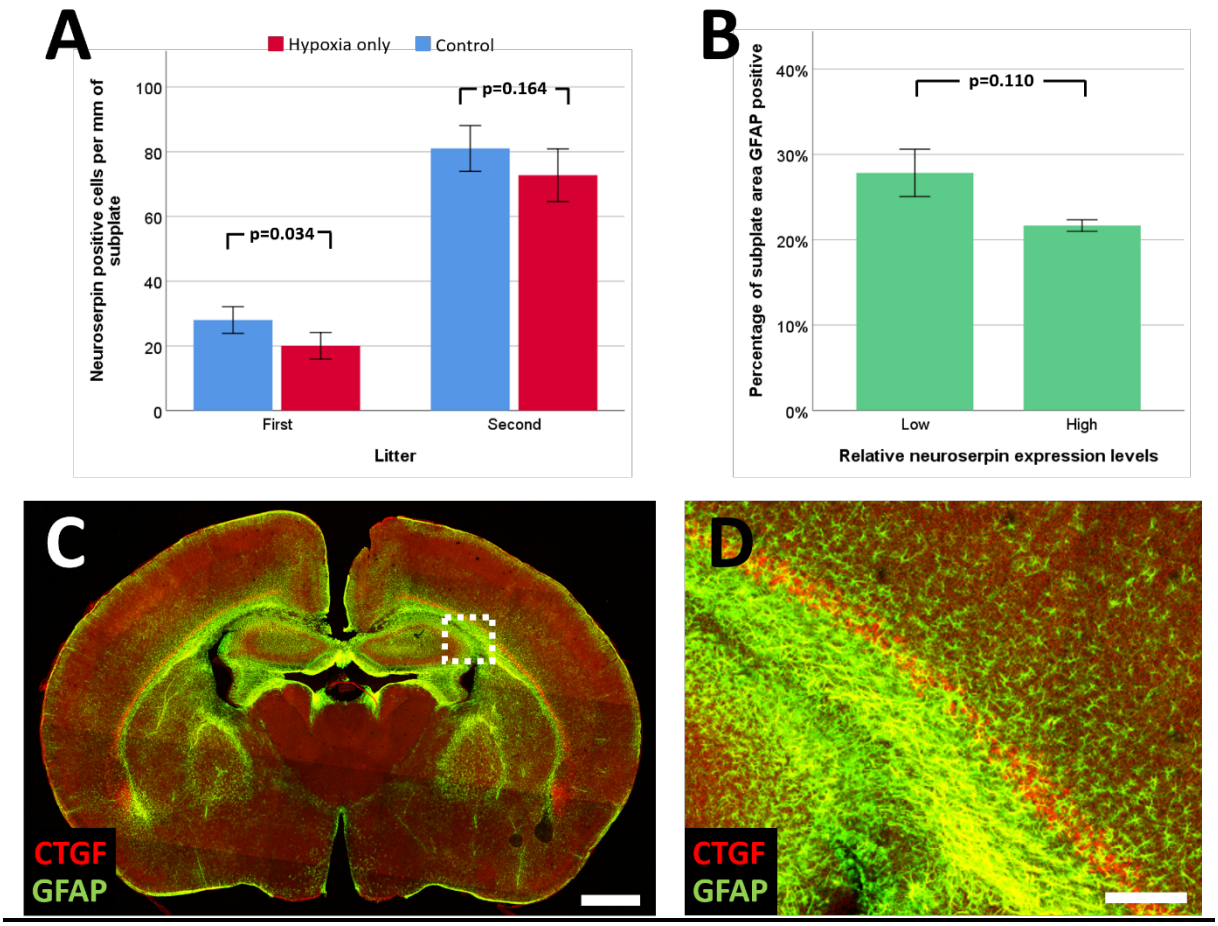

Figure 9. *Neuroserpin immunoreactive cortical neurons in P10 mice exposed to 90 min. of hypoxia only show reduced Neuroserpin expression.* ***A.*** *Comparing Neuroserpin expression in hypoxia only mouse pups and control littermates in two litters. Expression varies between litters due to different lots of primary antibody being used. P-value= 0.03 for both litters combined using ANOVA that controls for litters. Error bars show one standard error.* ***B.*** *Subplate GFAP expression when comparing the pup with the lowest and the pup with the highest subplate Neuroserpin expression. Error bars show one standard error.* ***C & D.*** *Coronal section of P10 mice stained for GFAP and CTGF (a subplate marker) with magnification of S1 subplate area (C). Co-localisation of GFAP and CTGF indicates GFAP expression in the subplate. C scale bar equals 1 mm. D scale bar equals 200 µm.*

fraction of L6b showing evidence of astrogliosis. The brain with low Neuroserpin expression showed a trend towards a greater proportion of subplate covered by astroglia than the brain with high Neuroserpin expression (27.8% vs. 21.7%, SEM_{Low}=2.8%, SD_{High}=0.7%; n=4 sections per sample; p=0.110) (**Figure 9.b-d**). This may suggest an inverse relationship between astrogliosis and Neuroserpin levels although this is merely a proof of concept. For more in-depth results on how

neonatal hypoxia can affected markers of inflammation and cellular damage please see further work from the lab by Millar (to be submitted as DPhil Thesis, 2019).

3.4 Potential mechanisms taking over the functions of Neuroserpin in the KO

Previous results showed that the knock-out of Neuroserpin in postnatal mice had no statistically significant effect on ischaemic area as a result of hypoxic-ischaemic encephalopathy. Existing literature had, however, suggested a neuroprotective effect of Neuroserpin in other adult rodent models of focal and global ischaemia. It was therefore proposed that redundancy mechanisms may

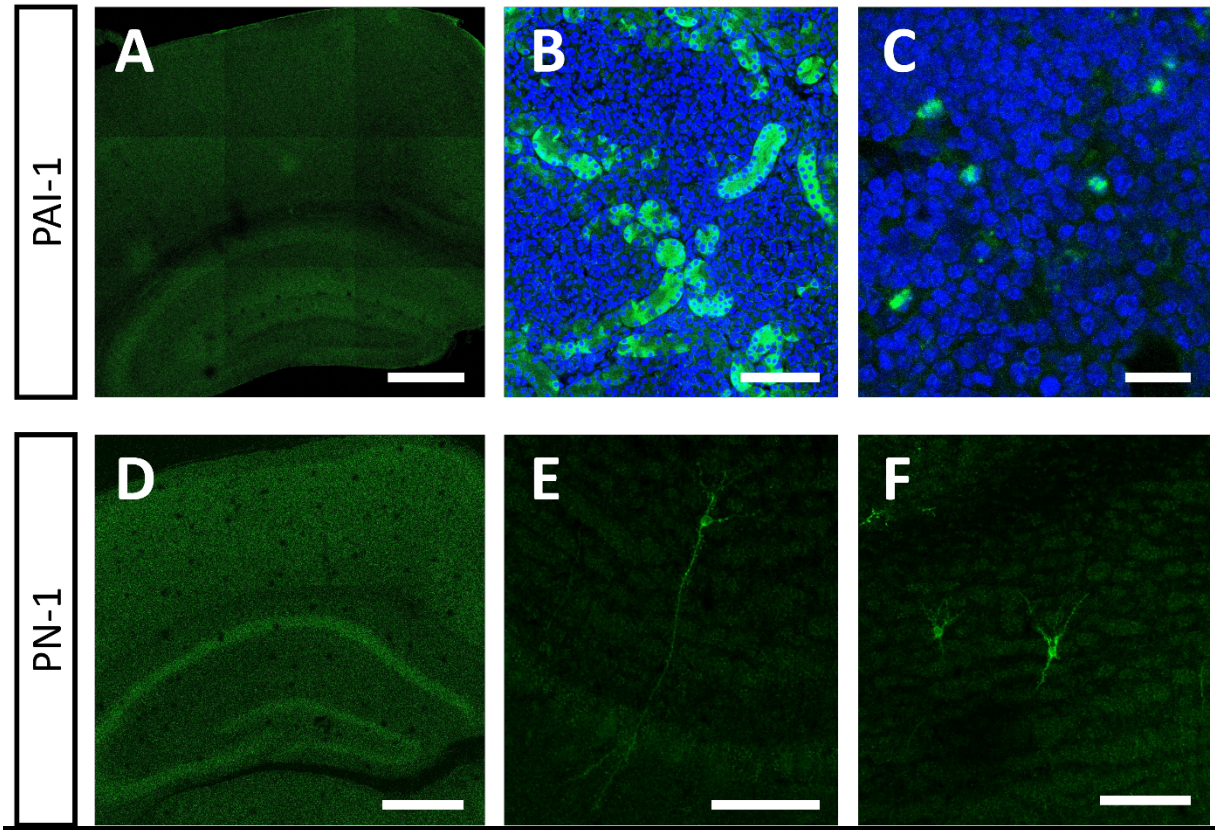

***Figure 10**. Potential mechanisms and proteins hypothesised to take over the functions of Neuroserpin show no cortical expression in the KO mouse. **A-C.** Fluorescent immunohistochemistry using PAI-1 primary antibody. **A.** Staining of cerebral cortex and hippocampus of Neuroserpin KO mouse at P10. Only background fluorescence visible. Scale bar equals 500 µm. **B.** Immunopositive control in kidney tissue (P10) with DAPI counterstain. Scale bar equals 100 µm. **C.** Positive control in lung tissue (P10) with DAPI counterstain. Scale bar equals 20 µm. **D-F.** Fluorescent immunohistochemistry using PN-1 primary antibody. **D.** Staining of cerebral cortex and hippocampus of Neuroserpin KO mouse at P10. Only background fluorescence visible. Scale bar equals 500 µm. **E&F.** Positive staining seen in individual neurons in olfactory bulbs of WT adult mice. Scale bars equal 100 µm.*

have a role in the postnatal mouse to take over some of Neuroserpin's roles and may in turn also convey some neuroprotective properties. The two most interesting proteins were plasminogen activator inhibitor 1 (PAI-1) and protease nexin 1 (PN-1) which also belong to the serpin protein

superfamily, albeit being in the phylogenic subgroup E rather than I, which is where Neuroserpin is found (Irving et al., 2000). These two are extracellular proteins with the ability to inhibit tissue plasminogen activator (tPA) as well as urokinase plasminogen activator (uPA) and thus have much in common with Neuroserpin (Law et al., 2006). Both, PAI-1 and PN-1, are found in human astrocytes in vivo and hence are prime candidates for potential redundancy mechanisms for Neuroserpin (Hultman et al., 2010). Their expression patterns in wild-type and Neuroserpin knock-out mice were therefore examined. PAI-1 showed no expression in postnatal mouse brains (**Figure 10**.**a**) and only showed positive immunofluorescence in mouse kidney and lung tissue (**Figure 10.b-c**). PN-1 staining was detected in the mouse brain, however, only in a few neurons in the olfactory bulbs (**Figure 10.e-f**). No staining beyond background fluorescence was detected in the cortex or the hippocampus (**Figure 10.d**). A lack of detection in both wild-type and knock-out tissue therefore makes redundancy mechanisms through these particular proteins unlikely.

3.5 Comparing neonatal human and mouse Neuroserpin expression

To ascertain how the data collected in mice correlates to humans one needs to first establish how Neuroserpin is expressed in human neonates. A temporal lobe of a neonatal brain at full-term (38 post-conceptual weeks) was obtained from the London Brain Bank (**Figure 11.a**). A section of temporal lobe was stained for Neuroserpin with adjacent sections being stained for cresyl violet (Nissl) and Alcian blue by Dr. István Adorján (**Figure 11**.**d-e**). The latter two stains aid in the identification of the individual cortical layers. Three different gyri of the temporal lobe were quantitatively examined, namely the superior, middle and inferior temporal gyrus (**Figure 11.c**). Neuroserpin expression was found in cells throughout the cerebral cortex and appeared to be similar in all temporal gyri. Cells staining for Neuroserpin showed axon- and dendrite-like projections indicating that similar to mice, Neuroserpin is mainly expressed by neurons (**Figure 11.c**). Neuroserpin positive cell densities were lowest in L4 and were highest in the adjacent L5. The subplate remnant could no longer be distinguished from the remainder of L6 at this developmental time point in the temporal gyri. Yet,

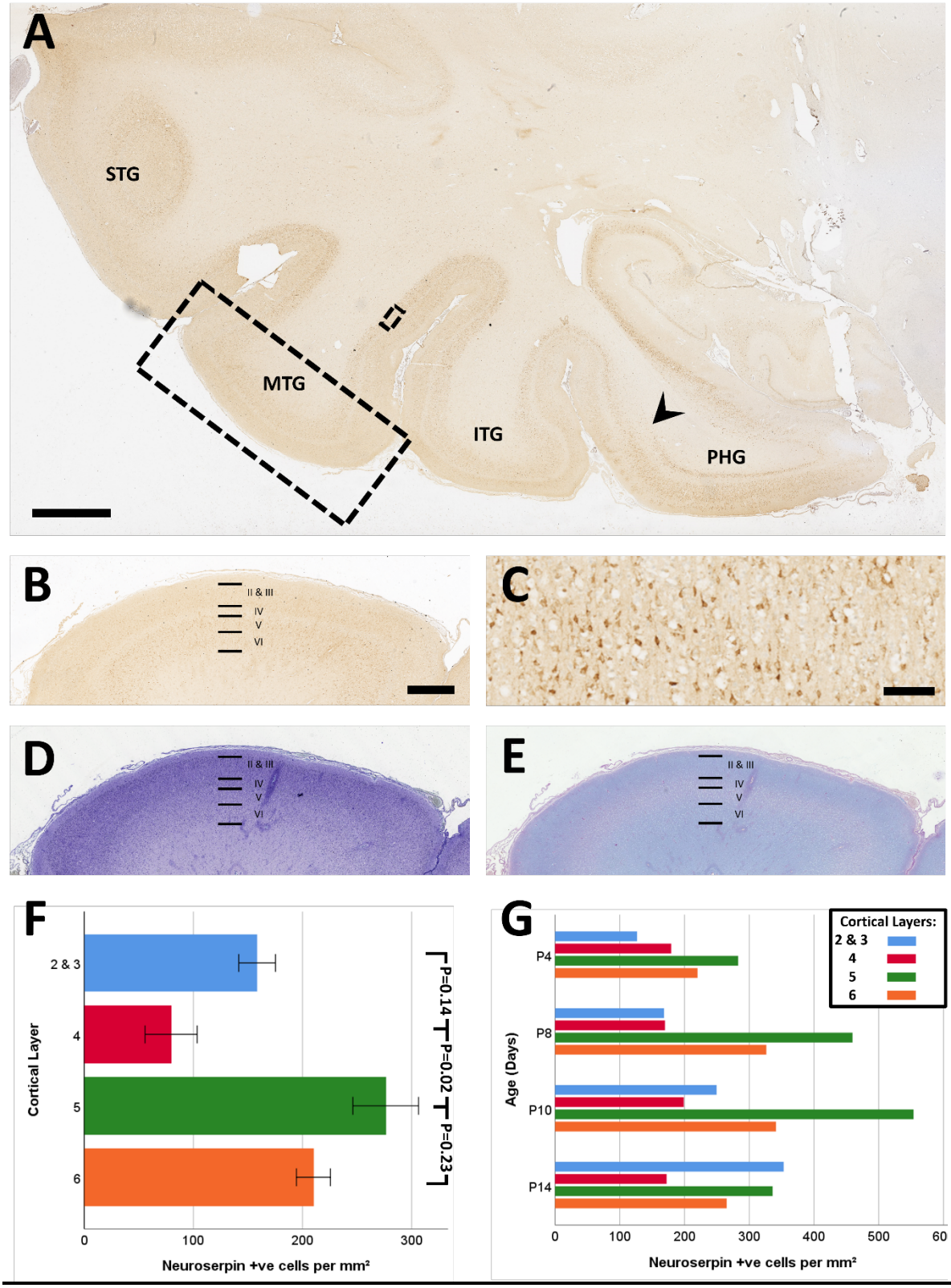

***Figure 11**. Human temporal lobe at 38 pcw (full-term) shows similar Neuroserpin expression pattern as P10 mouse brain. **A**. Temporal lobe stained for Neuroserpin. STG – superior temporal gyrus, MTG – middle temporal gyrus, ITG – inferior temporal gyrus, PHG – parahippocampal gyrus. Arrow denotes change in Neuroserpin expression pattern in the transition from the perirhinal gryus to the parahippocampal gyrus. Scale bar equals 3 mm. Sample and staining provided by István Adorján. **B.** Magnified middle temporal gyrus with Neuroserpin staining. Neuroserpin is expressed throughout all cortical layers with a visible reduction in L4 of the cortex. Scale bar equals 1 mm. **C**. Magnified area showing L6 Neuroserpin expressing cells in the lateral middle temporal gyrus. Scale bar equals 100 µm. **D.** Nissl staining of middle temporal gyrus. **E.** Alcian-blue staining of middle temporal gyrus which together with the nissl stain (D) allows for the identification of the cortical layers. **F.** Cell density*

of Neuroserpin positive cells in the respective cortical layers. One sample from each of the temporal gyri was included. Error bars indicate one standard error from the mean. ***G.*** *Expression pattern of Neuroserpin in mouse tissue of ages P4-P14. This allows for comparison between human and mouse expression. Human Neuroserpin expression at 38 pcw most closely resembles mouse expression at P10.*

there is a sudden point of transition in the posterior parahippocampal gyrus where at a dense layer of Neuroserpin expression arises at the base of L6 which may be evidence of a subplate remnant. Elsewhere L6 Neuroserpin positive cell densities are lower than those in L5, though still greater than those in L2/3. Overall, greater Neuroserpin expression in deeper cortical layers in comparison to more superficial ones was also confirmed by Adorján et al. (2019) using a similar approach.

One can now also compare these levels of expression in the full-term human brain to those observed during the developmental time series in mice (**Figure 6 & Figure 11.g**). To facilitate direct comparison the mouse L6a and L6b data were combined to create a single L6 data point. The relative cell densities of Neuroserpin positive cells seen in the human brain most closely resemble those of the P10 mouse brain (**Figure 11.g**). This time point is close to P8, which is when the mouse brain is generally assumed to most closely resemble the cortical structure and developmental stage of a human neonatal brain. Together with dense Neuroserpin expression in L6b of the posterior parahippocampal gyrus this suggests that overall Neuroserpin patterns are well conserved between these two species. Moreover, it increases the likelihood of translatability of the findings from this study to human neonates.

4. Discussion

4.1 Investigating neuroprotective properties of neuroserpin in neonatal models

My findings suggest that the lack of endogenous neuroserpin has no statistically significant effect on the extent of ischaemia caused by hypoxia brought about in the Rice-Vannucci model. There is no previous work directly investigating the effects of neuroserpin in neonatal hypoxic-ischaemic encephalopathy *in vivo*. My work can only be compared with *in vitro* studies as well as adult rodent studies. In vitro experiments have been conducted by two groups that have utilised cells obtained from foetal (Ma et al., 2012) or neonatal (Wang et al., 2015; Yang et al., 2016) rat brains to attempt to replicate *in vivo* conditions. These groups reported neuroprotective effects of Neuroserpin following oxygen-glucose deprivation and reoxygenation in the form of increased cell survival (Wang et al., 2015) as well as reduced inflammation (Yang et al., 2016) and excitotoxicity (Ma et al., 2012). Yet importantly, both groups used the administration of exogenous recombinant human Neuroserpin, thus likely increasing levels beyond those found in normal physiological conditions. So rather than compare a control wild-type condition with a condition in which Neuroserpin was lacking, these groups compared wild-type cells with cells exposed to an excess of Neuroserpin. Moreover, the complexity of the system is dramatically reduced *in vitro.* All groups dissociated the brain cells prior to plating thereby disrupting normal brain architecture and cellular interplay meaning that *in vivo* conditions were only poorly replicated.

4.2 Comparison to Neuroserpin's properties in adult stroke models

Due to the complexities of the pathological process in NHIE it may be more accurate to compare our work to other adult hypoxic-ischaemic insult models *in vivo*. One such approach is the middle cerebral artery occlusion (MCAO) that is used to model stroke in adult rodents. Some groups have explored the actions of Neuroserpin in this model either through the use of knock-out animals or by increasing availability either through exogenous administration or endogenous increase of expression. Using adult Neuroserpin knock-out mice Gelderblom et al. (2013) reported that KO mice had more

ischaemia, higher mortality and worse functional outcomes than wild-type controls following MCAO. Although no difference in total microglia numbers was found, a significant increase in activated, tumour-necrosis factor (TNF) secreting microglia was noted in KO mice. Microglial activation has frequently been associated with NHIE and increased activation is usually associated with poorer outcomes (Dommergues et al., 2003; Hagberg et al., 2015; McRae et al., 1995). Moreover, secretion of peptides belonging to the TNF family has also commonly been linked to increased damage, yet some neuroprotective effects have also been reported (Cammer and Zhang, 1999; Hagberg et al., 2015; Kichev et al., 2018; Pang et al., 2007). The maturity of glial cells as well as the sex of the animal may play an important role in determining the effect these cytokines (Cammer and Zhang, 1999; Kichev et al., 2018). Sex was not a factor that was controlled in our experiments and strategies could be devised to explore how it affects outcomes in our experimental setup. Unpublished work conducted in our lab further looked at Iba-1 expression (a microglial marker) following hypoxic ischaemic encephalopathy and found no statistically significant difference between KO and wild-type animals (Millar, to be submitted as DPhil thesis in 2019).

Asides from Gelderblom et al. (2013), three further studies explored Neuroserpin in models of adult stroke (Cinelli et al., 2001; Yepes et al., 2000; Zhang et al., 2002). Yepes et al. (2000) administered exogenous Neuroserpin following MCAO and found reduced ischaemia, decreased apoptosis and a reduction in basement membrane destruction. The same group also administered Neuroserpin in combination with tPA and reported a decrease in ischaemic volume in comparison to tPA administration only (Zhang et al., 2002). Yet, the joint use of tPA adds an important factor that prevents direct comparability with our results. A second group used overexpression of endogenous Neuroserpin to explore its effect in MCAO (Cinelli et al., 2001). Infarct size was again reduced which was attributed to reduced microglial activation and tPA (and uPA) activity. Interestingly, no alteration in endogenous tPA expression has been found in Neuroserpin KO mice indicating that alternative mechanisms can take over control to regulate expression (Madani et al., 2003). Nevertheless, tPA expression should also be examined in further studies of NHIE in Neuroserpin KO to determine if and

how it is affected. In summary, our results in neonatal mice do not mirror the neuroprotective effects of neuroserpin in adult mice. This may be attributed to a large array of factors ranging from the maturity of the brains, over differential tPA expression to differences in general susceptibilities to damage. Moreover, overexpression or administration of exogenous Neuroserpin has not been tested in any study thus far. Hence, it may be possible that protective properties are only exhibited if Neuroserpin is present at levels exceeding physiological expression.

4.3 Region and layer specific susceptibility to damage

Our work has also highlighted that various brain regions have divergent vulnerabilities to NHIE (Rice et al., 1981; Towfighi et al., 1997). The hippocampus and striatum are the most vulnerable whereas the cortex and thalamus are substantially less vulnerable. These areas also have distinct patterns of Neuroserpin expression, which however do not correlate to the extent of ischaemic damage. The cortex expresses substantial amounts of Neuroserpin and is moderately resistant to ischaemic damage. Unlike the striatum, which expresses no Neuroserpin and is far more susceptible to ischaemic damage. The thalamus shows similar resistance to the cortex yet only expresses Neuroserpin in its lateral portion. Moreover, the hippocampus has significantly greater Neuroserpin expression than the thalamus yet is significantly more vulnerable to ischaemic damage. Vulnerability to NHIE is most certainly a multifactorial characteristic and Neuroserpin's potential neuroprotective properties may be outweighed by other factors. Nevertheless, the hypothesis that it acts as a neuroprotective agent is significantly weakened by these observations.

Further studies have also investigated the susceptibility of various layers of the cortex to HIE (McQuillen et al., 2003; Mikhailova et al., 2017; Okusa et al., 2014; Sizonenko et al., 2003; Towfighi et al., 1997). The conclusions that were reached however diverged. Some groups found that the lower layers including the subplate (L6b) were particularly vulnerable (McQuillen et al., 2003; Mikhailova et al., 2017; Sizonenko et al., 2003; Towfighi et al., 1997). Yet, these findings were not confirmed by another group which reported that lower and upper layers were equally susceptible to damage (Okusa

et al., 2014). Regardless, neither conclusion lends support to the hypothesis that Neuroserpin has protective effects. This is because our data shows that at the time of the insult (P8) there is substantially more Neuroserpin expression in L6 and L5 than in L4 and L2/3. If Neuroserpin were to reduce the damage caused, one would expect that the upper layers would be more vulnerable than the lower ones. However, this is not the case in any of the aforementioned studies.

Comparing cell vulnerabilities between individual layers is nonetheless complicated by the fact that the neurons found in different cortical layers have varying degrees of maturity. The subplate neurons are amongst the earliest generated neurons of the cortex and they are the most mature cells in the cerebral cortex thus potentially behaving differently in response to insults than those of the upper cortical layers (Hoerder-Suabedissen and Molnár, 2015). This difference makes subplate cells more susceptible for excitatory amino acid lesions selectively at early stages of development (Ghosh et al., 1990). Importantly, maturity does not necessarily affect the different forms of cell death, namely apoptosis, necrosis and autophagy, seen in response to NHIE equally (Millar et al., 2017; Thornton et al., 2017a). It has been shown *in vitro* that an increase in maturity is negatively correlated with susceptibility to apoptotic cell death but positively to necrotic cell death as a result of excitotoxicity (McDonald et al., 1997). Depending on the interaction of neuron maturity, severity of injury and mode of cell death Neuroserpin may therefore retain some neuroprotective properties in deep layers by reducing susceptibility to excitotoxicity induced cell death.

4.4 Variability of subplate size and neuroserpin expression during development

A drawback of the use of adult models is that Neuroserpin expression is vastly different in the mature brain in comparison to the neonatal one. Timeseries have shown that it is expressed in a layer specific manner throughout the neonatal period when development continues in the rodent brain. Contrariwise, in the adult mouse Neuroserpin expression appears more homogenous across the different layers. Neuroserpin's initial differential expression in cortical layers may therefore point towards developmentally important functions that are no longer of significance in the adult brain. In

the NHIE model an upregulation of its expression may thus be prevented by overriding developmental programs. In addition, its reduced expression in the brain hemisphere of the ligated side may simply be attributed to cellular damage interfering with the machinery of protein synthesis. Likewise, in a model of ischaemic stroke Zhang et al. (2002) reported a reduction of Neuroserpin expression on the affected side thereby corroborating our results. Nevertheless, increased expression in the area around the ischaemic lesion has also been reported by others (Yepes et al., 2000).

In my study, Neuroserpin expression following NHIE was quantified in the subplate as it was proposed that this was a major site of extracellular Neuroserpin secretion (Kondo et al., 2015). However, during late brain development the subplate undergoes major changes as it drastically shrinks due to massive cell apoptosis in brains of mice and men (Hoerder-Suabedissen and Molnár, 2015; Price et al., 1997). Simultaneously, the brain and cortex continue to increase in size. Together, these effects may dramatically diminish the subplate's ability to secrete Neuroserpin in sufficient quantities to create a neuroprotective effect.

4.5 Comparison to clinically approved treatments for HIE

My study contributes to the body of knowledge that allows scientists and physicians to assess whether Neuroserpin is a clinically useful target to reduce the damage caused by NHIE. It can therefore be useful to compare proposed treatments to those that have already been clinically approved. In this case it would mean comparing the use of Neuroserpin to therapeutic hypothermia, currently the only approved therapy for NHIE. It may be hypothesised that Neuroserpin treatments would require at least similar protective effects to hypothermia in order to eventually gain clinical approval in the long-term and to warrant further investment into further research now.

Hypothermia showed a 30%-90% reduction in histological damage secondary to hypoxic insults in infant vertebrates ranging from rats to lambs (Bona et al., 1998; Gunn et al., 1997; Sirimanne et al., 1996; Wood et al., 2016). When looking at the effects of hypothermia specifically in the neonatal mouse model of NHIE similar results were achieved with reductions of neuronal damage in the range

of 60-80% (Reinboth et al., 2016; Rocha-Ferreira et al., 2018). These significant differences highlight the high utility of hypothermia in the treatment of NHIE. Potential neuroprotective effects of Neuroserpin are likely to be far from those seen in hypothermia. Should Neuroserpin have similarly pronounced effects these would have been detected with our experimental design with a power exceeding 80%. Albeit, unlikely to be a therapeutic option that can replace hypothermia, Neuroserpin may still have a role as an adjunct therapy. More subtle neuroprotective effects could not be excluded in our setup due to the variability that was observed. Many therapeutic options have been proposed to be introduced in conjunction with hypothermia, namely Xenon, Erythropoietin or Melatonin (McAdams and Juul, 2016) and Neuroserpin would therefore be no exception. Yet, the evidence provided by our work in the neonatal mouse model so far does not suggest any beneficial therapeutic potential.

Several future experimental avenues, however, remain to be explored. Neuroserpin's neuroprotective properties during increased bioavailability should be investigated either through an increase of endogenous secretion or administration of exogenous Neuroserpin. Moreover, other model organisms can be considered, highlighted by the observation that much hypoxic ischaemic encephalopathy research has been conducted in rats as well as in piglets and sheep (Davidson et al., 2015). Finally, alternate markers of damage, for example inflammation and apoptosis (Millar, to be submitted as DPhil thesis in 2019), should be used in order to detect more subtle variations in damage.

5. Limitations of Methods

5.1 Neuroserpin quantification

In the experiments presented in this thesis the level of neuroserpin expression was determined by quantifying the number of cells that were positive for primary neuroserpin antibody. Neuroserpin is a protein that is secreted into the extracellular environment. The numbers of Neuroserpin positive cells may not accurately reflect the absolute quantities of Neuroserpin present. It has been assumed that more Neuroserpin positive cells (NPCs) are equivalent to greater overall expression. Yet, the same number of NPCs may also be responsible for greater protein production and secretion. Our approach, therefore, fails to assess the total amount of protein expressed. An alternative method that has been previously employed in the lab was western blotting to quantify expression. This was only employed in entire brain hemispheres and did not find any statistically significant differences between the ligated and the non-ligated hemispheres. Furthermore, this approach was deemed unsuitable for our analysis focused on subplate expression levels of neuroserpin. Although microdissections of the subplate could be achieved, a reliable western blot would require tissue from large numbers of animals due to the small size of the subplate. As this tissue would be unsuitable for any additional analysis and the data would only be used as tertiary confirmation, this approach was not undertaken.

Moreover, antibodies from different producers or batches may bind with varying affinity thereby affecting the count. We normally used the same batch of antibody throughout individual experiments to allow for comparability. In the hypoxia-only experimental setup different batches of antibody had to be used for the two litters examined which led to significant inter-litter variability in the antibody stain. However, the use of controls within each litter allowed for comparison of the two results. Finally, NPCs were counted based on stain intensity and size using an automatic approach that was subsequently cross-checked manually. This technique is advantageous as it does not only assess a random sample within the region of interest of a histological section but quantifies the entire region.

Nonetheless, the risk of false negatives is slightly elevated using this method as some neurons may not fulfil the size requirements set.

5.2 Rice-Vannucci model and the quantification of ischaemic damage

One of the key limitations of the methods employed was the variability observed in the outcomes of the modified Rice-Vannucci model. High variability was already described when the model was being developed and has persisted despite optimisation attempts over the last three decades (Edwards et al., 2017; Rice et al., 1981). To some extent, this makes the Rice-Vannucci approach an accurate model of human neonatal hypoxic ischaemic encephalopathy as short and long term outcomes vary significantly in the clinical settings (de Vries and Jongmans, 2010). However, this lack of consistency means that the risks of type I and type II errors are drastically increased when employing the Rice-Vannucci model in research.

In our setup, ischaemic brain damage was only observed when the hypoxic period exceeded 30 minutes thus indicating a minimum hypoxic time requirement. A maximum time of hypoxia also arose from the necessity of maintaining a post-procedure survival of more than 80% due to home office project license requirements. This survival limit was being approached at 45 minutes of hypoxia and in order to give sufficient margin the hypoxic period was limited to 40 minutes. At this duration of hypoxia, a significant proportion of brains showed no evidence of ischaemic damage thus creating a skew in the dataset. The dataset could be normalised by also undertaking analysis of the brains with ischaemic damage alone. Nonetheless, the high variability of the Rice-Vannucci model, also noted by many established groups (Edwards et al., 2017; Okusa et al., 2014; Sheldon et al., 1998), has led to relatively high standard errors which would have prevented the detection of subtle changes in the given sample size. Finally, the TTC used to stain non-ischaemic areas of the brain has been found to show inaccuracies in differentiating healthy and ischaemic tissue (Benedek et al., 2006). It may overstate the ischaemic area as healthy neurons can be found in TTC-negative areas. Recovery of tissue in the penumbra of the ischaemic lesion may also occur.

5.3 Human tissue stainings

Neuroserpin, Nissl and Alcian blue tissue stains of human developmental brain tissue samples were obtained for analysis (Adorján et al., 2019). One of the key difficulties encountered was a counter stain of haematoxylin in the diaminobenzidine (DAB) stained Neuroserpin samples. Blue haematoxylin was able to highlight cell nuclei. Yet, it interfered with the quantification of neuroserpin positive cells as overlapping blue and brown staining obscured cell boundaries making accurate quantification impossible. Moreover, substantial background staining created a further risk for false positives.

It was therefore determined that repeat staining would be required. However, as no adjacent sections were available to the already stained samples new sections were also required. In the time available no successful procedure could be established, thereby limiting analysis to individual haematoxylin free samples.

6. Bibliography

Adorján, I., Tyler, T., Bhaduri, A, Demharter, S, Finszter, C., Bako, M., Sebok, O., Nowakowski, T., Khodosevich, K., Mollgard, K., et al. (2019). Neuroserpin expression during human brain development and in adult brain revealed by immunohistochemistry and single cell RNA sequencing. Journal of Anatomy.

Alake, O., Hardman, S., and Chakkarapani, E. (2018). Managing hypoxic ischaemic encephalopathy in term newborn infant. Paediatrics and Child Health *28*, 399–404.

Azzopardi, D. V., Strohm, B., Edwards, A. D., Dyet, L., Halliday, H. L., Juszczak, E., et al. (2009). Moderate Hypothermia to Treat Perinatal Asphyxial Encephalopathy. *N Engl J Med*, *361*(14), 1349–1358. doi:10.1056/NEJMoa0900854

Azzopardi, D., Strohm, B., Marlow, N., Brocklehurst, P., Deierl, A., Eddama, O., et al. (2014). Effects of Hypothermia for Perinatal Asphyxia on Childhood Outcomes. *N Engl J Med*, *371*(2), 140–149. doi:10.1056/NEJMoa1315788

Bano, S., Chaudhary, V., and Garga, U.C. (2017). Neonatal Hypoxic-ischemic Encephalopathy: A Radiological Review. Journal of Pediatric Neurosciences *12*, 1–6.

Benedek, A., Móricz, K., Jurányi, Z., Gigler, G., Lévay, G., Hársing, L.G., Mátyus, P., Szénási, G., and Albert, M. (2006). Use of TTC staining for the evaluation of tissue injury in the early phases of reperfusion after focal cerebral ischemia in rats. Brain Research *1116*, 159–165.

Bona, E., Hagberg, H., Løberg, E.M., Bågenholm, R., and Thoresen, M. (1998). Protective Effects of Moderate Hypothermia after Neonatal Hypoxia-Ischemia: Short- and Long-Term Outcome. Pediatric Research *43*, 738.

Boutilier, R.G. (2001). Mechanisms of cell survival in hypoxia and hypothermia. J. Exp. Biol. *204*, 3171.

Cammer, W., and Zhang, H. (1999). Maturation of oligodendrocytes is more sensitive to TNFα than is survival of precursors and immature oligodendrocytes. Journal of Neuroimmunology *97*, 37–42.

Cheng, Y., Loh, Y.P., and Birch, N.P. (2017). Neuroserpin Attenuates H2O2-Induced Oxidative Stress in Hippocampal Neurons via AKT and BCL-2 Signaling Pathways. Journal of Molecular Neuroscience *61*, 123–131.

Cinelli, P., Madani, R., Tsuzuki, N., Vallet, P., Arras, M., Zhao, C.N., Osterwalder, T., Rülicke, T., and Sonderegger, P. (2001). Neuroserpin, a Neuroprotective Factor in Focal Ischemic Stroke. Molecular and Cellular Neuroscience *18*, 443–457.

Cole, J.W., Naj, A.C., O'Connell, J.R., Stine, O.C., Sorkin, J.D., Wozniak, M.A., Stern, B.J., Yepes, M., Lawrence, D.A., Reinhart, L.J., et al. (2007). Neuroserpin polymorphisms and stroke risk in a biracial population: the stroke prevention in young women study. BMC Neurology *7*, 37–37.

Davidson, J.O., Wassink, G., van den Heuij, L.G., Bennet, L., and Gunn, A.J. (2015). Therapeutic Hypothermia for Neonatal Hypoxic-Ischemic Encephalopathy - Where to from Here? Frontiers in Neurology *6*, 198–198.

Dommergues, M.-A., Plaisant, F., Verney, C., and Gressens, P. (2003). Early microglial activation following neonatal excitotoxic brain damage in mice: a potential target for neuroprotection. Neuroscience *121*, 619–628.

Edwards, A.B., Feindel, K.W., Cross, J.L., Anderton, R.S., Clark, V.W., Knuckey, N.W., and Meloni, B.P. (2017). Modification to the Rice-Vannucci perinatal hypoxic-ischaemic encephalopathy model in the P7 rat improves the reliability of cerebral infarct development after 48hours. Journal of Neuroscience Methods *288*, 62–71.

Gelderblom, M., Neumann, M., Ludewig, P., Bernreuther, C., Krasemann, S., Arunachalam, P., Gerloff, C., Glatzel, M., and Magnus, T. (2013). Deficiency in Serine Protease Inhibitor Neuroserpin Exacerbates Ischemic Brain Injury by Increased Postischemic Inflammation. PLOS ONE *8*, e63118.

von Gertten, C., Morales, A.F., Holmin, S., Mathiesen, T., and Nordqvist, A.-C.S. (2005). Genomic responses in rat cerebral cortex after traumatic brain injury. BMC Neuroscience *6*, 69–69.

Ghosh, A., Antonini, A., McConnell, S.K., and Shatz, C.J. (1990). Requirement for subplate neurons in the formation of thalamocortical connections. Nature *347*, 179.

Gu, R.P., Fu, L.L., Jiang, C.H., Xu, Y.F., Wang, X., and Yu, J. (2015). Retina Is Protected by Neuroserpin from Ischemic/Reperfusion-Induced Injury Independent of Tissue-Type Plasminogen Activator. PLOS ONE *10*, e0130440.

Gunn, A.J., Gunn, T.R., de Haan, H.H., Williams, C.E., and Gluckman, P.D. (1997). Dramatic neuronal rescue with prolonged selective head cooling after ischemia in fetal lambs. J Clin Invest *99*, 248–256.

Hagberg, H., Mallard, C., Ferriero, D.M., Vannucci, S.J., Levison, S.W., Vexler, Z.S., and Gressens, P. (2015). The role of inflammation in perinatal brain injury. Nature Reviews. Neurology *11*, 192–208.

Hastings, G.A., Coleman, T.A., Haudenschild, C.C., Stefansson, S., Smith, E.P., Barthlow, R., Cherry, S., Sandkvist, M., and Lawrence, D.A. (1997). Neuroserpin, a Brain-associated Inhibitor of Tissue Plasminogen Activator Is Localized Primarily in Neurons: IMPLICATIONS FOR THE REGULATION OF MOTOR LEARNING AND NEURONAL SURVIVAL. Journal of Biological Chemistry *272*, 33062–33067.

Hoerder-Suabedissen, A., and Molnár, Z. (2015). Development, evolution and pathology of neocortical subplate neurons. Nature Reviews Neuroscience *16*, 133.

Hultman, K., Blomstrand, F., Nilsson, M., Wilhelmsson, U., Malmgren, K., Pekny, M., Kousted, T., Jern, C., and Tjärnlund-Wolf, A. (2010). Expression of plasminogen activator inhibitor-1 and protease nexin-1 in human astrocytes: Response to injury-related factors. Journal of Neuroscience Research *88*, 2441–2449.

Irving, J.A., Pike, R.N., Lesk, A.M., and Whisstock, J.C. (2000). Phylogeny of the Serpin Superfamily: Implications of Patterns of Amino Acid Conservation for Structure and Function. Genome Research *10*, 1845–1864.

Ishigami, S., Sandkvist, M., Tsui, F., Moore, E., Coleman, T.A., and Lawrence, D.A. (2007). Identification of a novel targeting sequence for regulated secretion in the serine protease inhibitor neuroserpin. The Biochemical Journal *402*, 25–34.

Kichev, A., Baburamani, A.A., Vontell, R., Gressens, P., Burkly, L., Thornton, C., and Hagberg, H. (2018). TWEAK Receptor Deficiency Has Opposite Effects on Female and Male Mice Subjected to Neonatal Hypoxia-Ischemia. Frontiers in Neurology *9*, 230–230.

Kondo, S., Al-Hasani, H., Hoerder-Suabedissen, A., Wang, W.Z., and Molnár, Z. (2015). Secretory function in subplate neurons during cortical development. Frontiers in Neuroscience *9*, 100.

Kumar, A., and Ragg, H. (2008). Ancestry and evolution of a secretory pathway serpin. BMC Evolutionary Biology *8*, 250–250.

Law, R.H.P., Zhang, Q., McGowan, S., Buckle, A.M., Silverman, G.A., Wong, W., Rosado, C.J., Langendorf, C.G., Pike, R.N., Bird, P.I., et al. (2006). An overview of the serpin superfamily. Genome Biology *7*, 216–216.

Lebeurrier, N., Liot, G., Lopez-Atalaya, J.P., Orset, C., Fernandez-Monreal, M., Sonderegger, P., Ali, C., and Vivien, D. (2005). The brain-specific tissue-type plasminogen activator inhibitor, neuroserpin, protects neurons against excitotoxicity both in vitro and in vivo. Molecular and Cellular Neuroscience *30*, 552–558.

Lee, A.C., Kozuki, N., Blencowe, H., Vos, T., Bahalim, A., Darmstadt, G.L., Niermeyer, S., Ellis, M., Robertson, N.J., Cousens, S., et al. (2013). Intrapartum-related neonatal encephalopathy incidence and impairment at regional and global levels for 2010 with trends from 1990. Pediatric Research *74*, 50.

Levine, S. (1960). Anoxic-Ischemic Encephalopathy in Rats. The American Journal of Pathology *36*, 1–17.

Liang, W., Chuan-Zhen, L., Qiang, D., Jian, Q., Hui-Min, R., and Bao-Guo, X. (2004). Reductions in mRNA of the neuroprotective agent, neuroserpin, after cerebral ischemia/reperfusion in diabetic rats. Brain Research *1015*, 175–180.

Ma, J., Yu, D., Tong, Y., and Mao, M. (2012). Effect of neuroserpin in a neonatal hypoxic-ischemic injury model ex vivo. Biological Research *45*, 357–362.

Madani, R., Kozlov, S., Akhmedov, A., Cinelli, P., Kinter, J., Lipp, H.-P., Sonderegger, P., and Wolfer, D.P. (2003). Impaired explorative behavior and neophobia in genetically modified mice lacking or overexpressing the extracellular serine protease inhibitor neuroserpin. Molecular and Cellular Neuroscience *23*, 473–494.

Mathews, K.S., McLaughlin, D.P., Ziabari, L.H., Toner, C.C., Street, P.C., Hisgrove, E., Bezzina, E.L., and Stamford, J.A. (2000). Rapid quantification of ischaemic injury and cerebroprotection in brain slices using densitometric assessment of 2,3,5-triphenyltetrazolium chloride staining. Journal of Neuroscience Methods *102*, 43–51.

McAdams, R.M., and Juul, S.E. (2016). Neonatal Encephalopathy: Update on Therapeutic Hypothermia and Other Novel Therapeutics. Clinics in Perinatology *43*, 485–500.

McDonald, J.W., Behrens, M.I., Chung, C., Bhattacharyya, T., and Choi, D.W. (1997). Susceptibility to apoptosis is enhanced in immature cortical neurons. Brain Research *759*, 228–232.

McQuillen, P.S., Sheldon, R.A., Shatz, C.J., and Ferriero, D.M. (2003). Selective Vulnerability of Subplate Neurons after Early Neonatal Hypoxia-Ischemia. J. Neurosci. *23*, 3308.

McRae, A., Gilland, E., Bona, E., and Hagberg, H. (1995). Microglia activation after neonatal hypoxic-ischemia. Developmental Brain Research *84*, 245–252.

Mikhailova, A., Sunkara, N., and McQuillen, P.S. (2017). Unbiased Quantification of Subplate Neuron Loss following Neonatal Hypoxia-Ischemia in a Rat Model. Developmental Neuroscience *39*, 171–181.

Millar, L. (2019). Characterisation of Neuroserpin Protein Expression Throughout Development and Investigation of Putative Neuroprotective Properties in Rodent Models of Neonatal Hypoxia Ischaemia.

Millar, L.J., Shi, L., Hoerder-Suabedissen, A., and Molnár, Z. (2017). Neonatal Hypoxia Ischaemia: Mechanisms, Models, and Therapeutic Challenges. Frontiers in Cellular Neuroscience *11*, 78.

Nair, J., and Kumar, V.H.S. (2018). Current and Emerging Therapies in the Management of Hypoxic Ischemic Encephalopathy in Neonates. Children (Basel, Switzerland) *5*, 99.

Okusa, C., Oeschger, F., Ginet, V., Wang, W.-Z., Hoerder-Suabedissen, A., Matsuyama, T., Truttmann, A.C., and Molnár, Z. (2014). Subplate in a rat model of preterm hypoxia–ischemia. Annals of Clinical and Translational Neurology *1*, 679–691.

Osterwalder, T., Contartese J., Stoeckli E. T., Kuhn T. B., and Sonderegger P. (1996). Neuroserpin, an axonally secreted serine protease inhibitor. The EMBO Journal *15*, 2944–2953.

Pang, Y., Zheng, B., Fan, L.-W., Rhodes, P.G., and Cai, Z. (2007). IGF-1 protects oligodendrocyte progenitors against TNFα-induced damage by activation of PI3K/Akt and interruption of the mitochondrial apoptotic pathway. Glia *55*, 1099–1107.

Price, D.J., Aslam, S., Tasker, L., and Gillies, K. (1997). Fates of the earliest generated cells in the developing murine neocortex. Journal of Comparative Neurology *377*, 414–422.

Reinboth, B.S., Köster, C., Abberger, H., Prager, S., Bendix, I., Felderhoff-Müser, U., and Herz, J. (2016). Endogenous hypothermic response to hypoxia reduces brain injury: Implications for modeling hypoxic-ischemic encephalopathy and therapeutic hypothermia in neonatal mice. Experimental Neurology *283*, 264–275.

Rice, J.E., Vannucci, R.C., and Brierley, J.B. (1981). The influence of immaturity on hypoxic-ischemic brain damage in the rat. Annals of Neurology *9*, 131–141.

Rocha-Ferreira, E., Vincent, A., Bright, S., Peebles, D.M., and Hristova, M. (2018). The duration of hypothermia affects short-term neuroprotection in a mouse model of neonatal hypoxic ischaemic injury. PloS One *13*, e0199890–e0199890.

Ruegg, M.A., Stoeckli, E.T., Kuhn, T.B., Heller, M., Zuellig, R., and Sonderegger, P. (1989). Purification of axonin-1, a protein that is secreted from axons during neurogenesis. The EMBO Journal *8*, 55–63.

Schindelin, J., Arganda-Carreras, I., Frise, E., Kaynig, V., Longair, M., Pietzsch, T., Preibisch, S., Rueden, C., Saalfeld, S., Schmid, B., et al. (2012). Fiji: an open-source platform for biological-image analysis. Nature Methods *9*, 676–682.

Schrimpf, S.P., Bleiker, A.J., Brecevic, L., Kozlov, S.V., Berger, P., Osterwalder, T., Krueger, S.R., Schinzel, A., and Sonderegger, P. (1997). Human Neuroserpin (PI12): cDNA Cloning and Chromosomal Localization to 3q26. Genomics *40*, 55–62.

Semple, B.D., Blomgren, K., Gimlin, K., Ferriero, D.M., and Noble-Haeusslein, L.J. (2013). Brain development in rodents and humans: Identifying benchmarks of maturation and vulnerability to injury across species. Progress in Neurobiology *106–107*, 1–16.

Sheldon, R.A., Sedik, C., and Ferriero, D.M. (1998). Strain-related brain injury in neonatal mice subjected to hypoxia–ischemia. Brain Research *810*, 114–122.

Sinha, B., Wu, Q., Li, W., Tu, Y., Sirianni, A.C., Chen, Y., Jiang, J., Zhang, X., Chen, W., Zhou, S., et al. (2018). Protection of melatonin in experimental models of newborn hypoxic-ischemic brain injury through MT1 receptor. Journal of Pineal Research *64*, e12443.

Sirimanne, E.S., Blumberg, R.M., Bossano, D., Gunning, M., Edwards, A.D., Gluckman, P.D., and Williams, C.E. (1996). The Effect of Prolonged Modification of Cerebral Temperature on Outcome after Hypoxic-Ischemic Brain Injury in the Infant Rat. Pediatric Research *39*, 591.

Sizonenko, S.V., Sirimanne, E., Mayall, Y., Gluckman, P.D., Inder, T., and Williams, C. (2003). Selective Cortical Alteration after Hypoxic-Ischemic Injury in the Very Immature Rat Brain. Pediatric Research *54*, 263.

Sofroniew, M.V. (2009). Molecular dissection of reactive astrogliosis and glial scar formation. Trends in Neurosciences *32*, 638–647.

Sorrells, S.F., Paredes, M.F., Cebrian-Silla, A., Sandoval, K., Qi, D., Kelley, K.W., James, D., Mayer, S., Chang, J., Auguste, K.I., et al. (2018). Human hippocampal neurogenesis drops sharply in children to undetectable levels in adults. Nature *555*, 377–381.

Stoeckli, E.T., LEMKIN Peter F., KUHN Thomas B., RUEGG Markus A., HELLER Martin, and SONDEREGGER Peter (1989). Identification of proteins secreted from axons of embryonic dorsal-root-ganglia neurons. European Journal of Biochemistry *180*, 249–258.

Thornton, C., Leaw, B., Mallard, C., Nair, S., Jinnai, M., and Hagberg, H. (2017a). Cell Death in the Developing Brain after Hypoxia-Ischemia. Frontiers in Cellular Neuroscience *11*, 248.

Thornton, C., Baburamani, A.A., Kichev, A., and Hagberg, H. (2017b). Oxidative stress and endoplasmic reticulum (ER) stress in the development of neonatal hypoxic-ischaemic brain injury. Biochemical Society Transactions *45*, 1067–1076.

Tjärnlund-Wolf, A., Olsson, S., Jood, K., Blomstrand, C., and Jern, C. (2011). No evidence for an association between genetic variation at the SERPINI1 locus and ischemic stroke. Journal of Neurology *258*, 1885.

Towfighi, J., Mauger, D., Vannucci, R.C., and Vannucci, S.J. (1997). Influence of age on the cerebral lesions in an immature rat model of cerebral hypoxia–ischemia: a light microscopic study. Developmental Brain Research *100*, 149–160.

Volpe, J.J. (2001). Perinatal brain injury: From pathogenesis to neuroprotection. Mental Retardation and Developmental Disabilities Research Reviews *7*, 56–64.

de Vries, L.S., and Jongmans, M.J. (2010). Long-term outcome after neonatal hypoxic-ischaemic encephalopathy. Arch Dis Child Fetal Neonatal Ed *95*, F220.

Wang, L., Zhang, Y., Asakawa, T., Li, W., Han, S., Li, Q., Xiao, B., Namba, H., Lu, C., and Dong, Q. (2015). Neuroprotective Effect of Neuroserpin in Oxygen-Glucose Deprivation- and Reoxygenation-Treated Rat Astrocytes In Vitro. PLOS ONE *10*, e0123932.

Wood, T., Osredkar, D., Puchades, M., Maes, E., Falck, M., Flatebø, T., Walløe, L., Sabir, H., and Thoresen, M. (2016). Treatment temperature and insult severity influence the neuroprotective effects of therapeutic hypothermia. Scientific Reports *6*, 23430.

Yang, X., Asakawa, T., Han, S., Liu, L., Li, W., Wu, W., Luo, Y., Cao, W., Cheng, X., Xiao, B., et al. (2016). Neuroserpin Protects Rat Neurons and Microglia-Mediated Inflammatory Response Against Oxygen-Glucose Deprivation- and Reoxygenation Treatments in an In Vitro Study. Cellular Physiology and Biochemistry *38*, 1472–1482.

Yepes, M., Sandkvist, M., Wong, M.K.K., Coleman, T.A., Smith, E., Cohan, S.L., and Lawrence, D.A. (2000). Neuroserpin reduces cerebral infarct volume and protects neurons from ischemia-induced apoptosis. Blood *96*, 569.

Yepes, M., Roussel, B.D., Ali, C., and Vivien, D. (2009). Tissue-type plasminogen activator in the ischemic brain: more than a thrombolytic. Trends in Neurosciences *32*, 48–55.

Zhang, Z., Zhang Li, Yepes Manuel, Jiang Quan, Li Qingjiang, Arniego Polly, Coleman Timothy A., Lawrence Daniel A., and Chopp Michael (2002). Adjuvant Treatment With Neuroserpin Increases the Therapeutic Window for Tissue-Type Plasminogen Activator Administration in a Rat Model of Embolic Stroke. Circulation *106*, 740–745.